

Evolution of Circumstellar Disks and Planet Formation



Wladimir Lyra
New Mexico State University

Current Funding



AAG – 2020, 2021



XRP - 2023

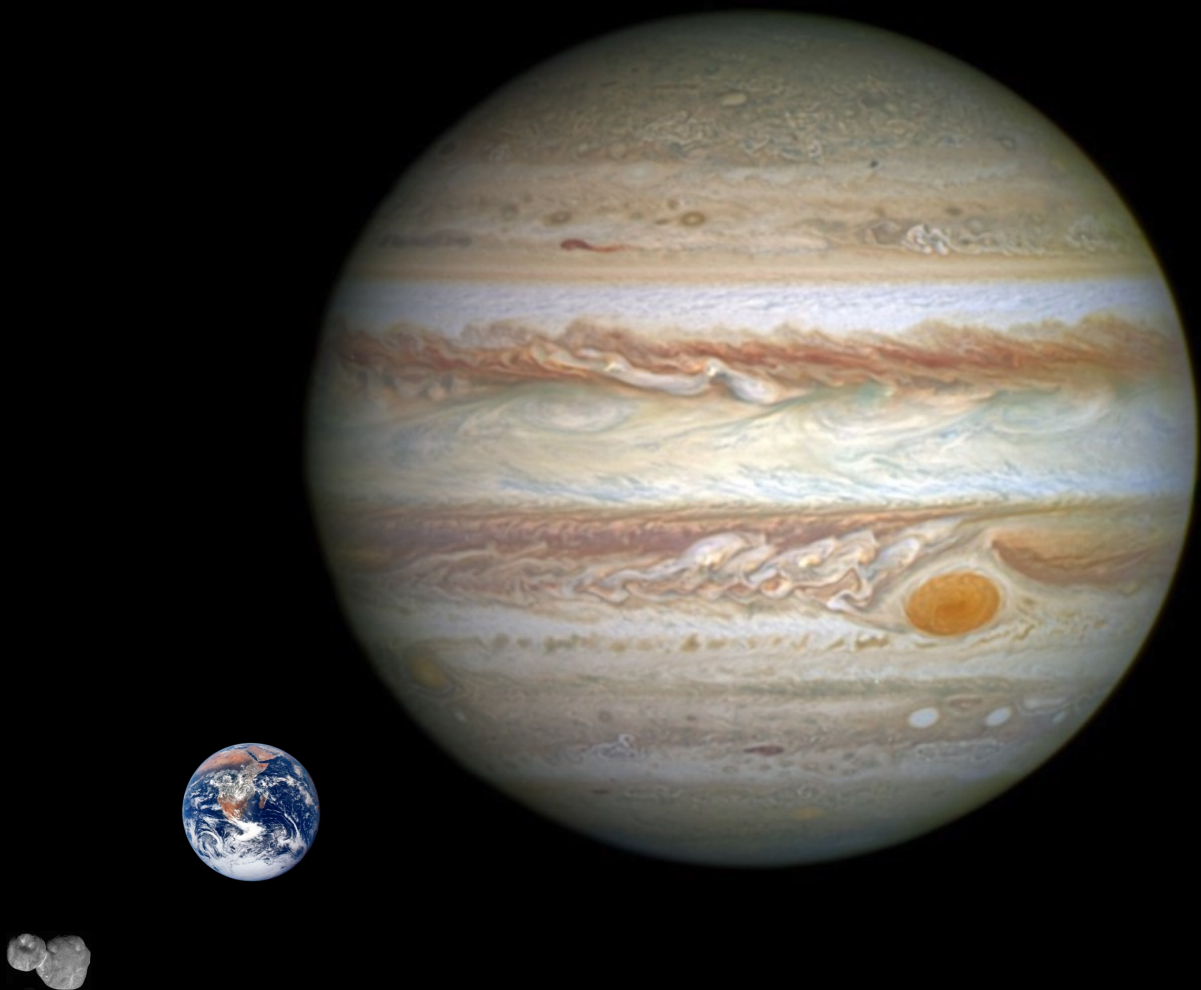
EW – 2021, 2022, 2023

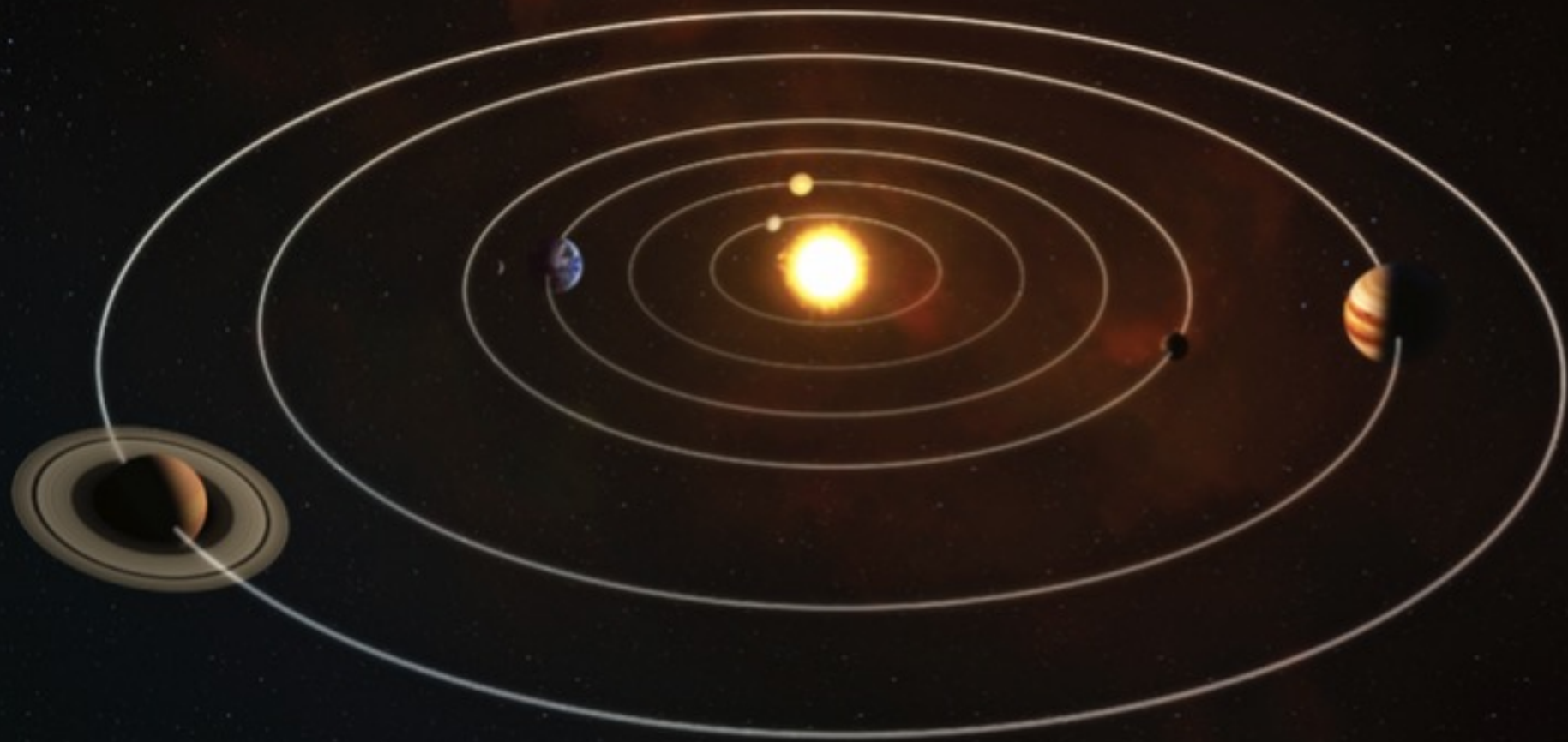
TCAN – 2020

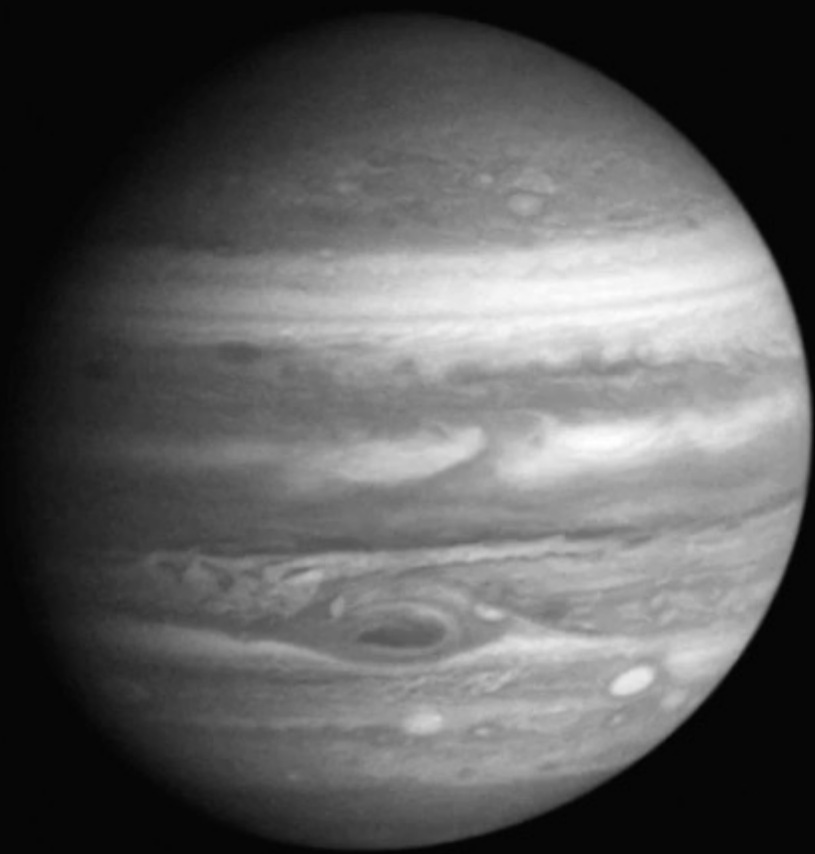
Computational Facilities



Planet Formation











Betelgeuse

Bellatrix

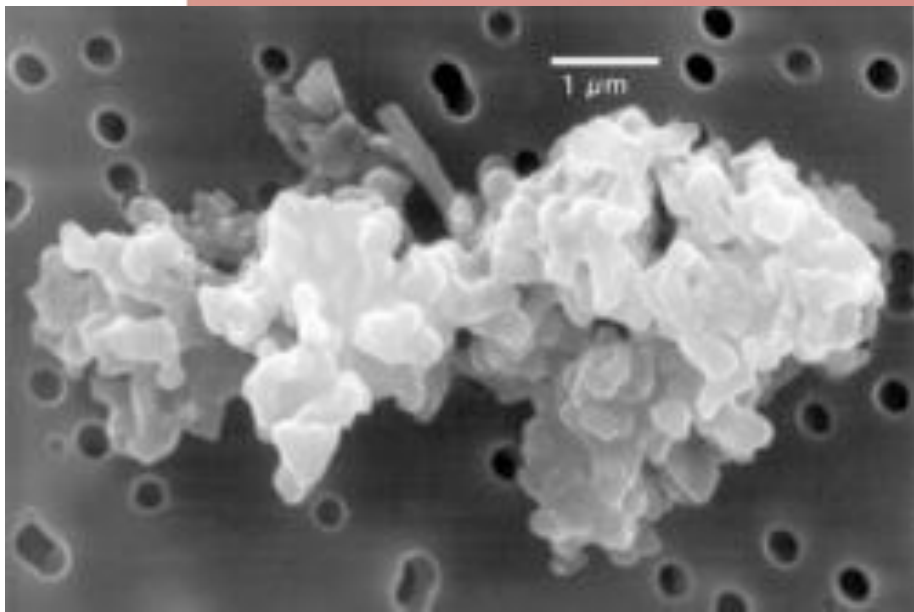
Orion's Belt

Orion Nebula

Rigel

Saiph







Circumstellar/Protoplanetary Disks



PP disk fact sheet

Density: $10^{13} - 10^{15} \text{ cm}^{-3}$
(Air: 10^{21} cm^{-3})

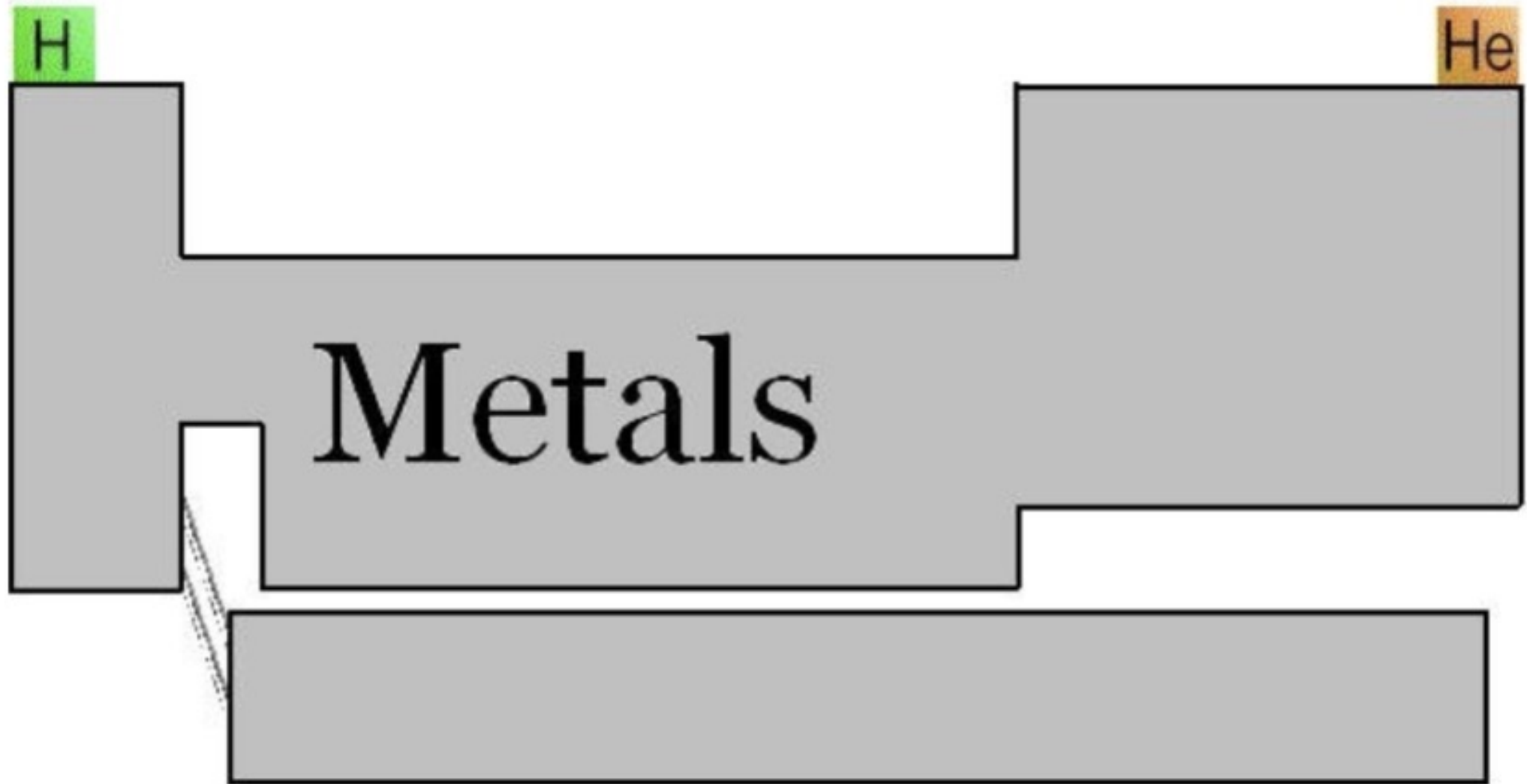
Temperature: 10-1000 K

Scale: 0.1-100AU

Mass: $10^{-3} - 10^{-1} M_{\text{sun}}$

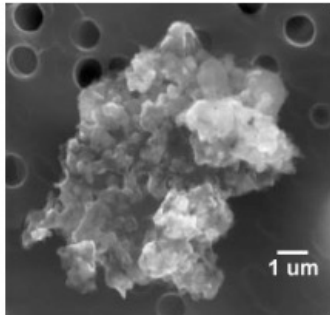
Composition: 5:2 H_2 -He
mixture. 1% metals.

The Astronomer's Periodic Table



Planet Formation

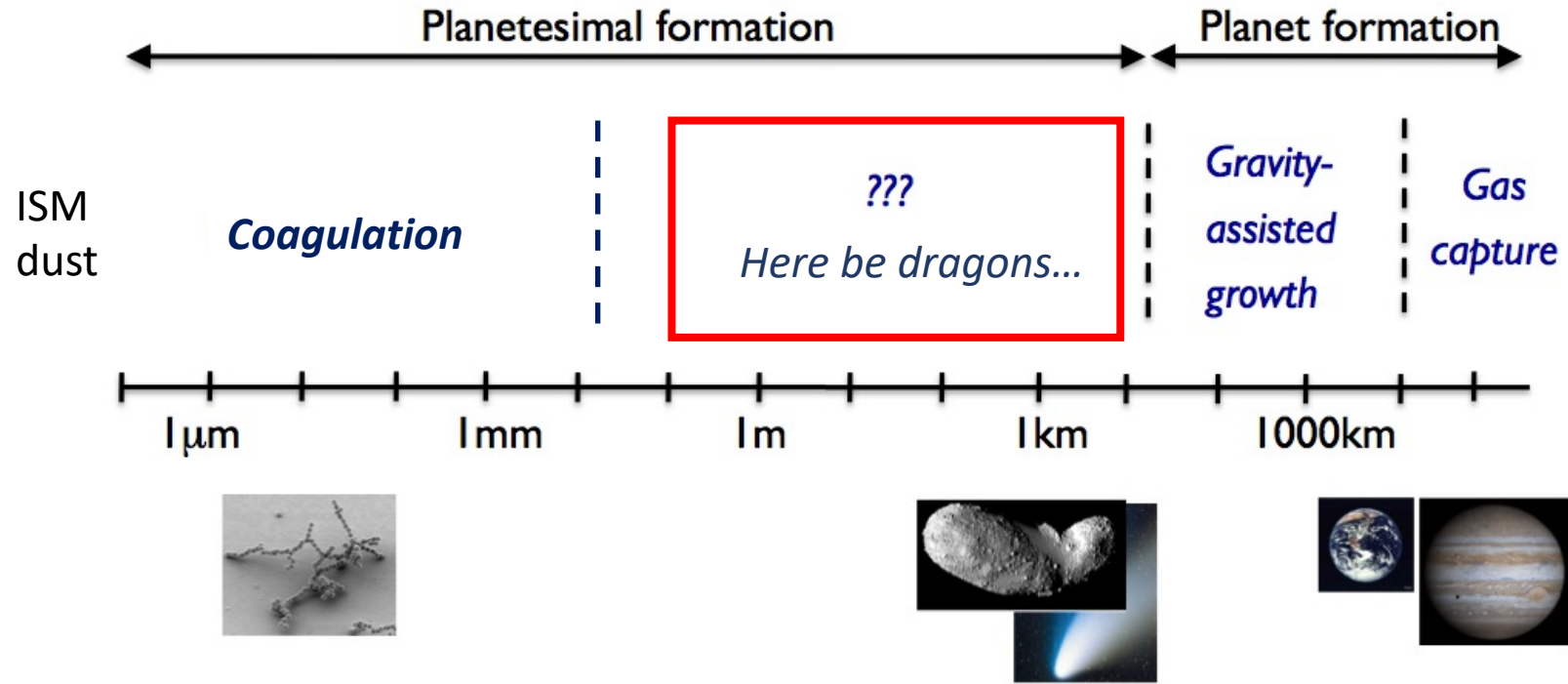
“Planets form in disks of gas and dust”



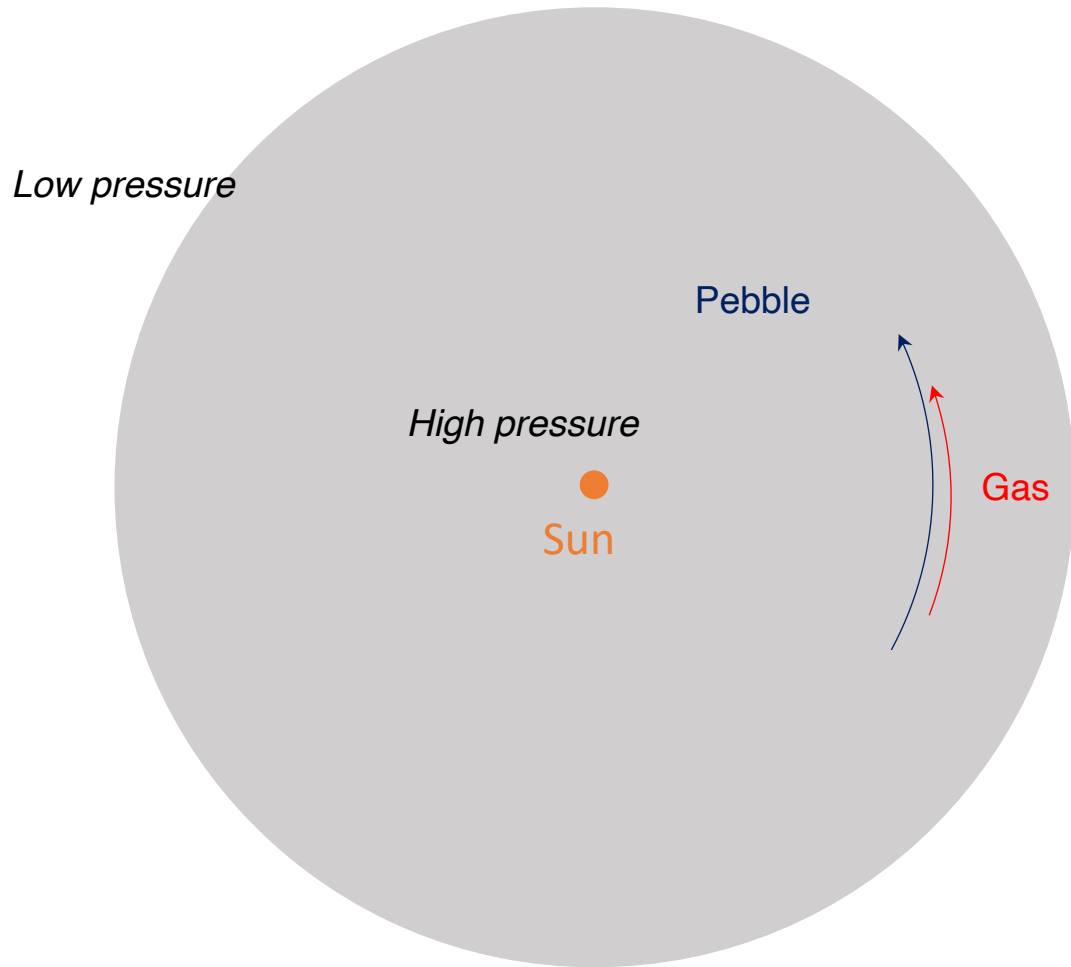
— ***A miracle happens*** —▶



Dust evolution



Headwind and Dust Drift



The **gas** has some pressure support (sub-Keplerian).

The **pebbles** do not feel gas pressure (Keplerian).

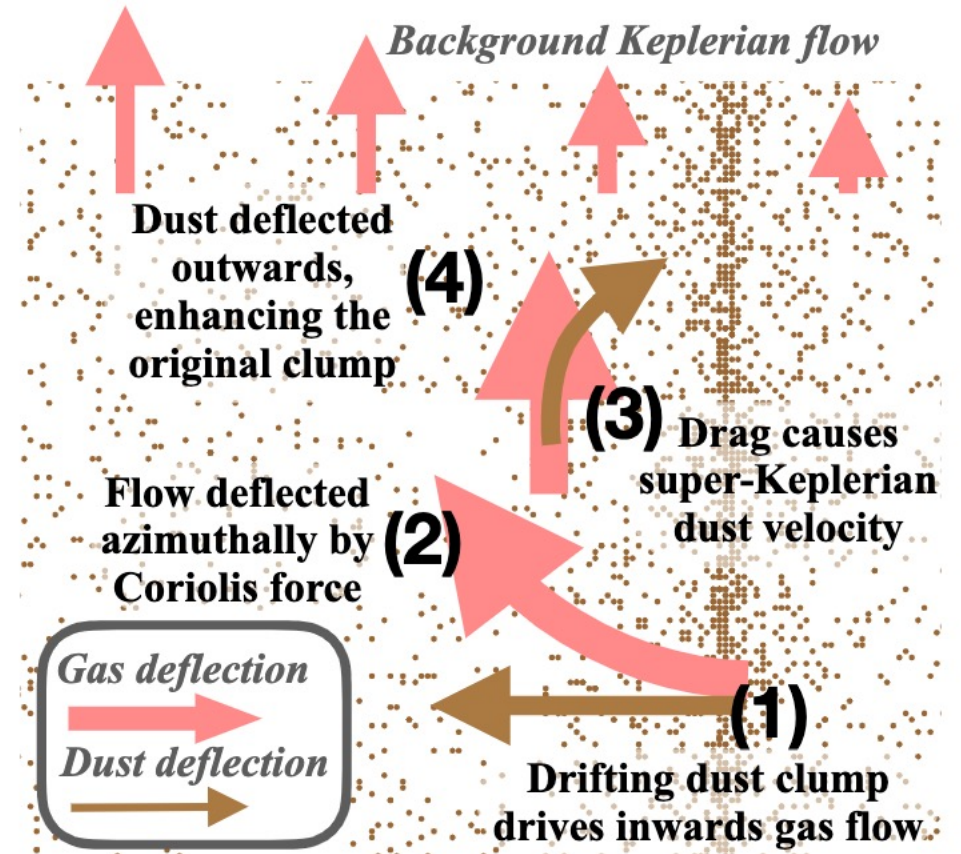
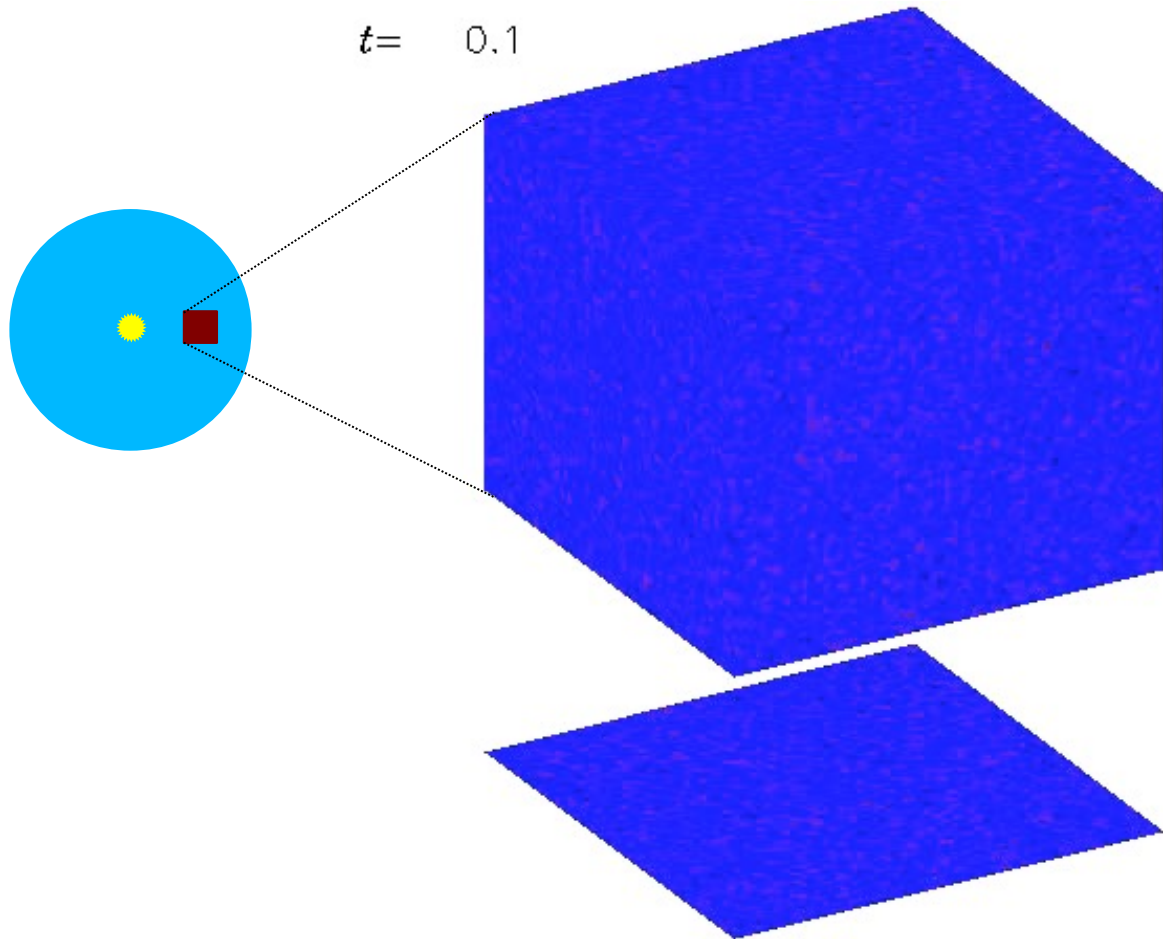
Dust coagulation and drift

Dust particle
coagulation
and radial drift

F. Brauer, C.P. Dullemond
Th. Henning

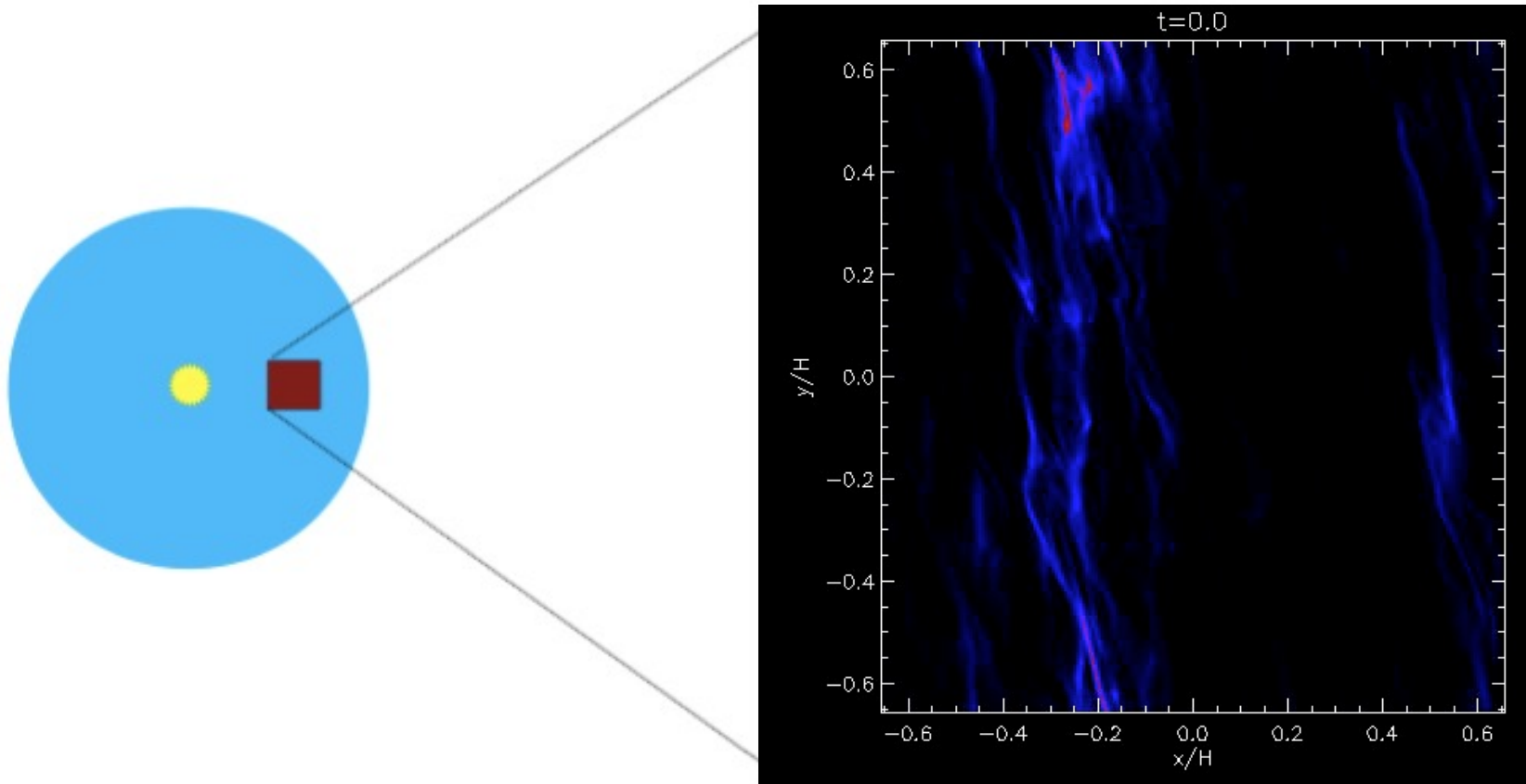
Streaming Instability

The dust drift is hydrodynamically unstable



Lesur et al. (2022)

Gravitational collapse into planetesimals



Johansen et al. (2007)

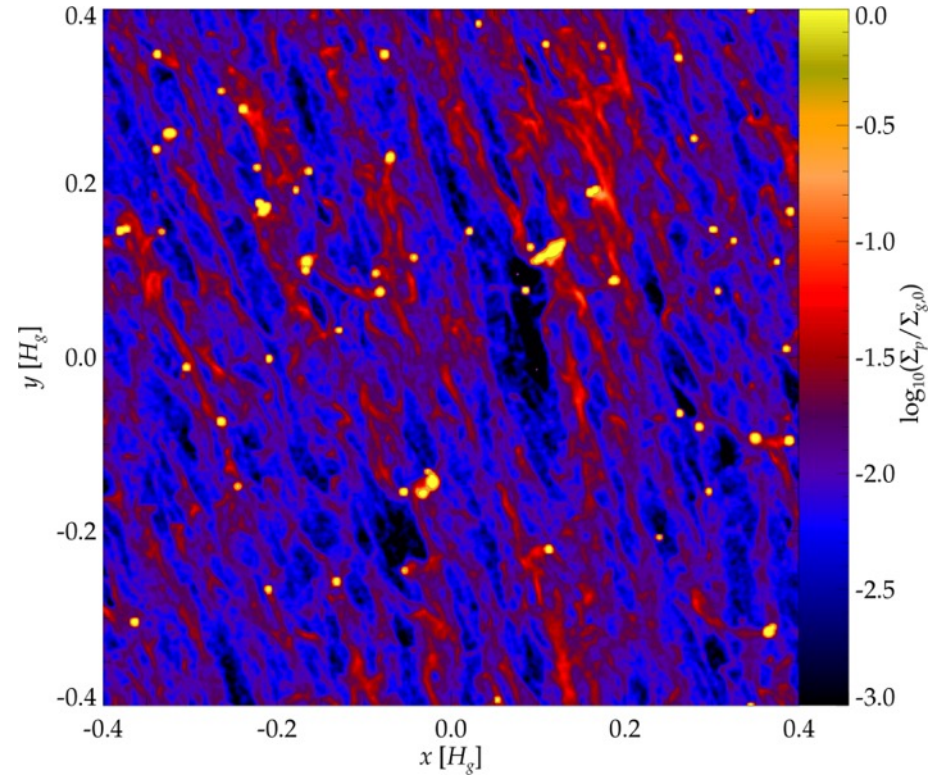
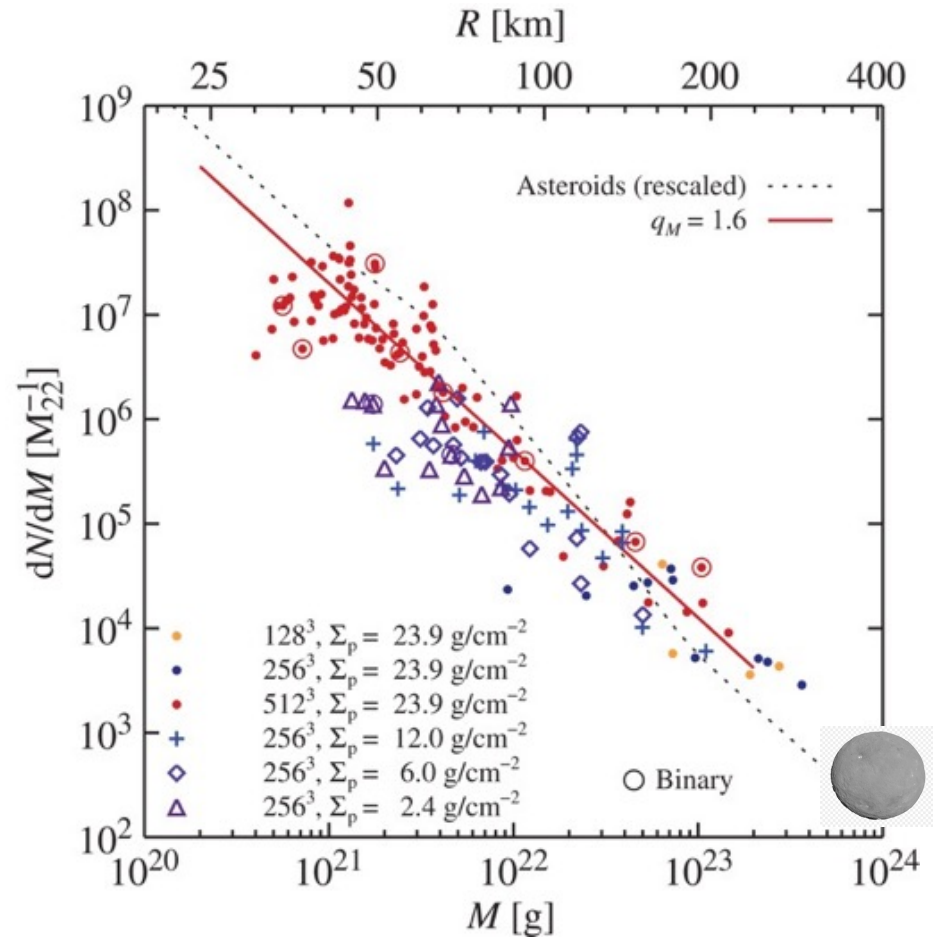


nature
astronomy

Fingerprints of
streaming instability

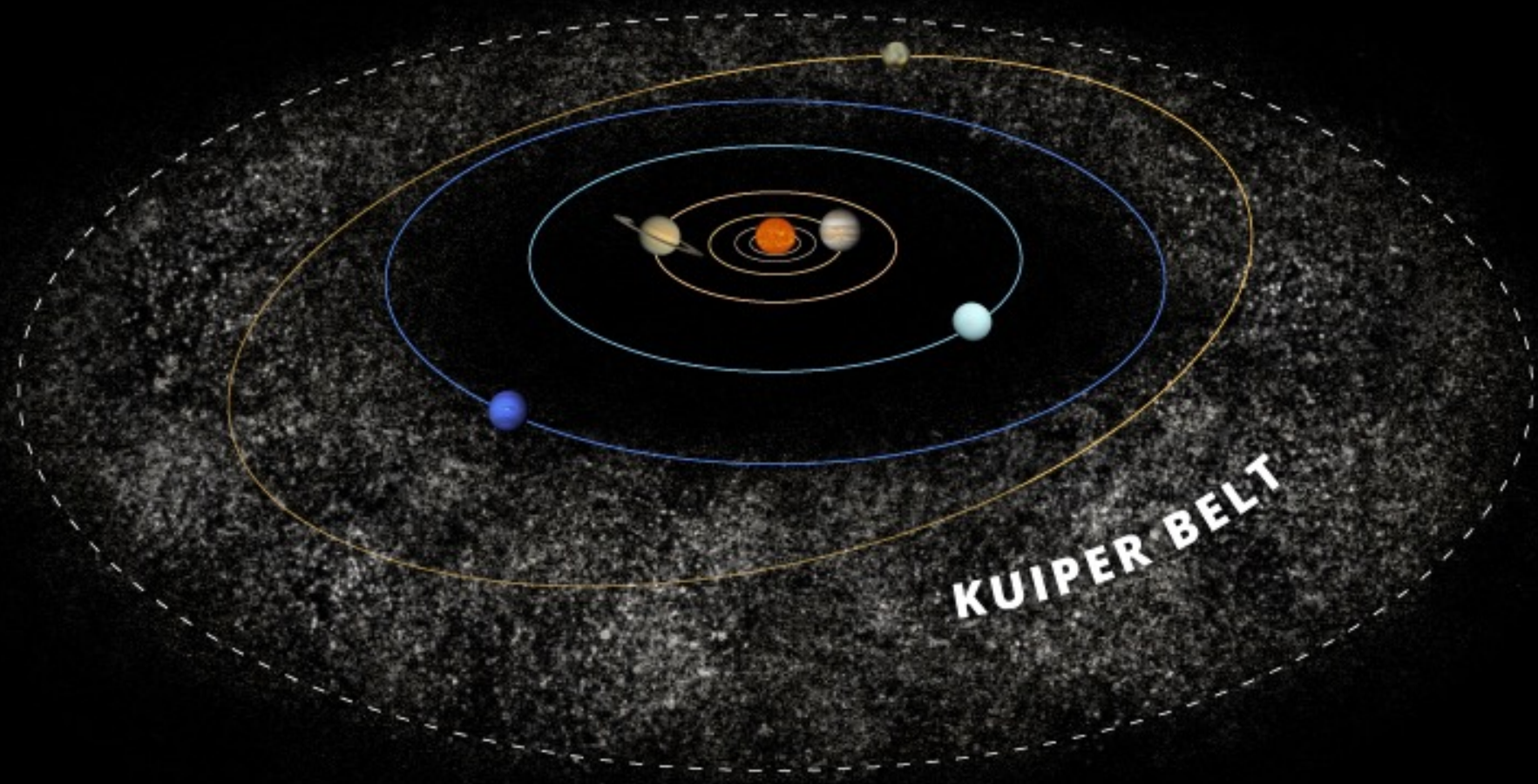
**How can we verify the
streaming instability
hypothesis?**

Planetesimal Formation

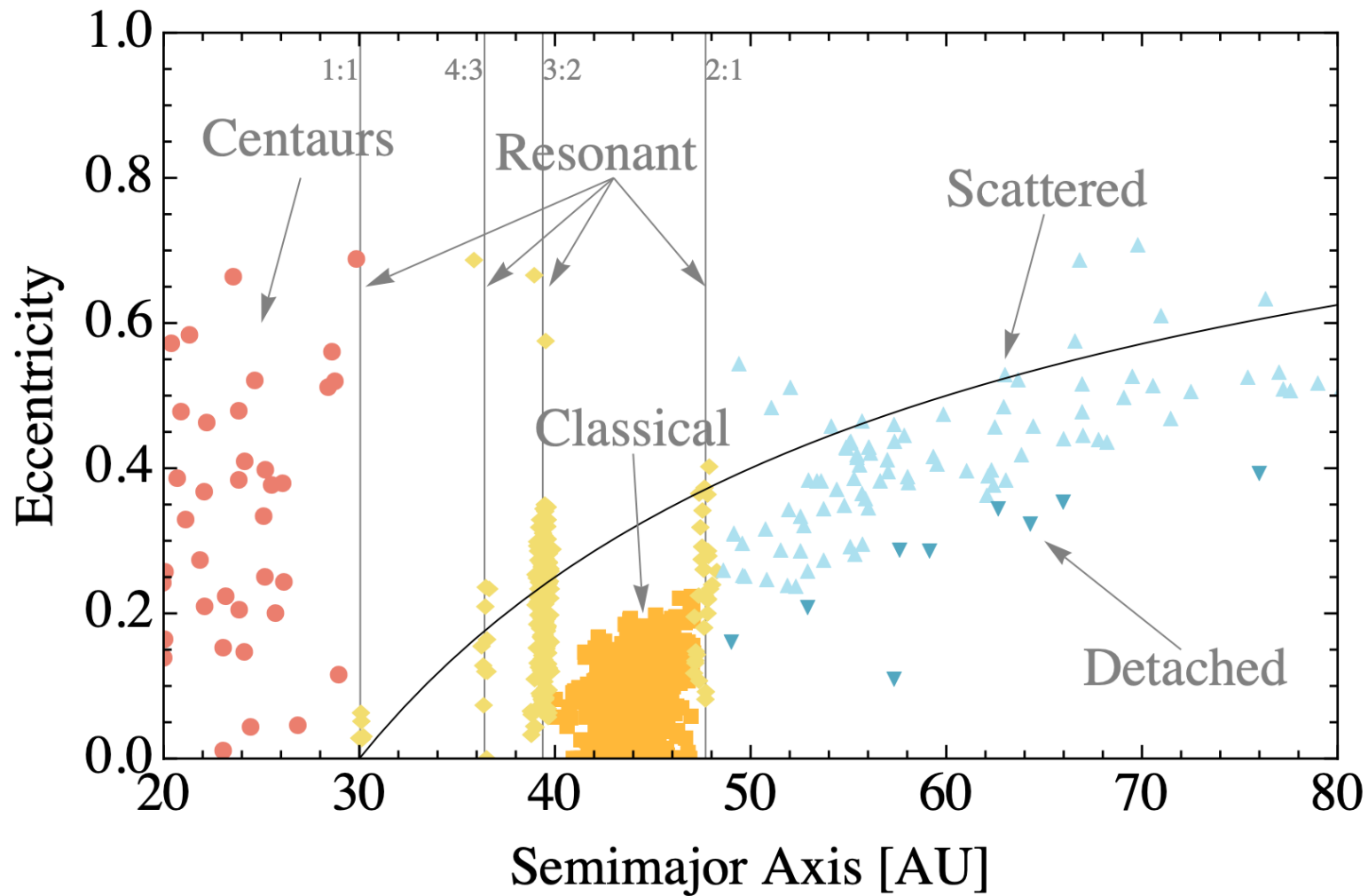


Initial mass function consistent with mass distribution of asteroid belt. Slope 1.6



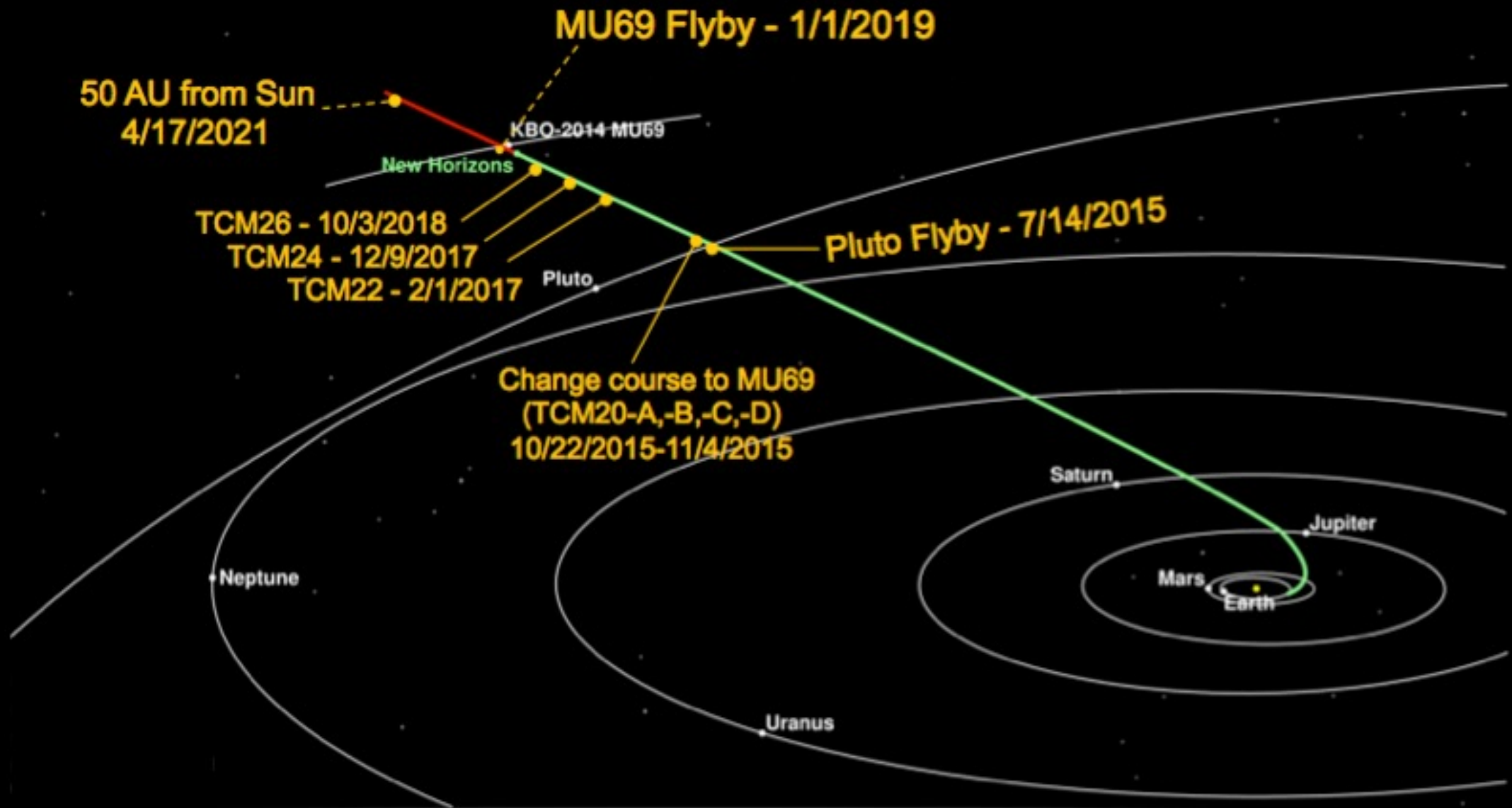


Structure of the Kuiper Belt

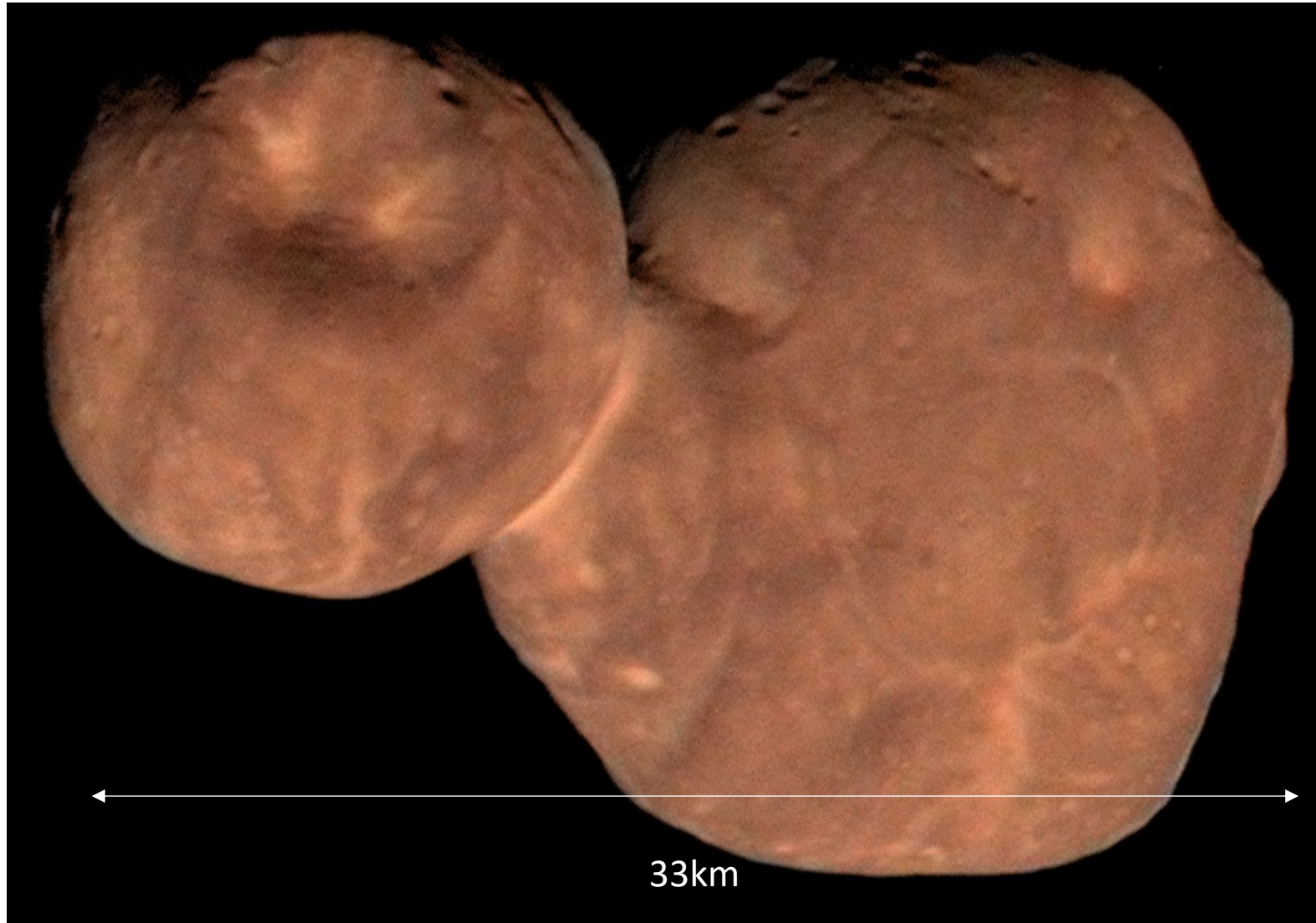


Classicals: Presumably
pristine planetesimals

New Horizons Trajectory

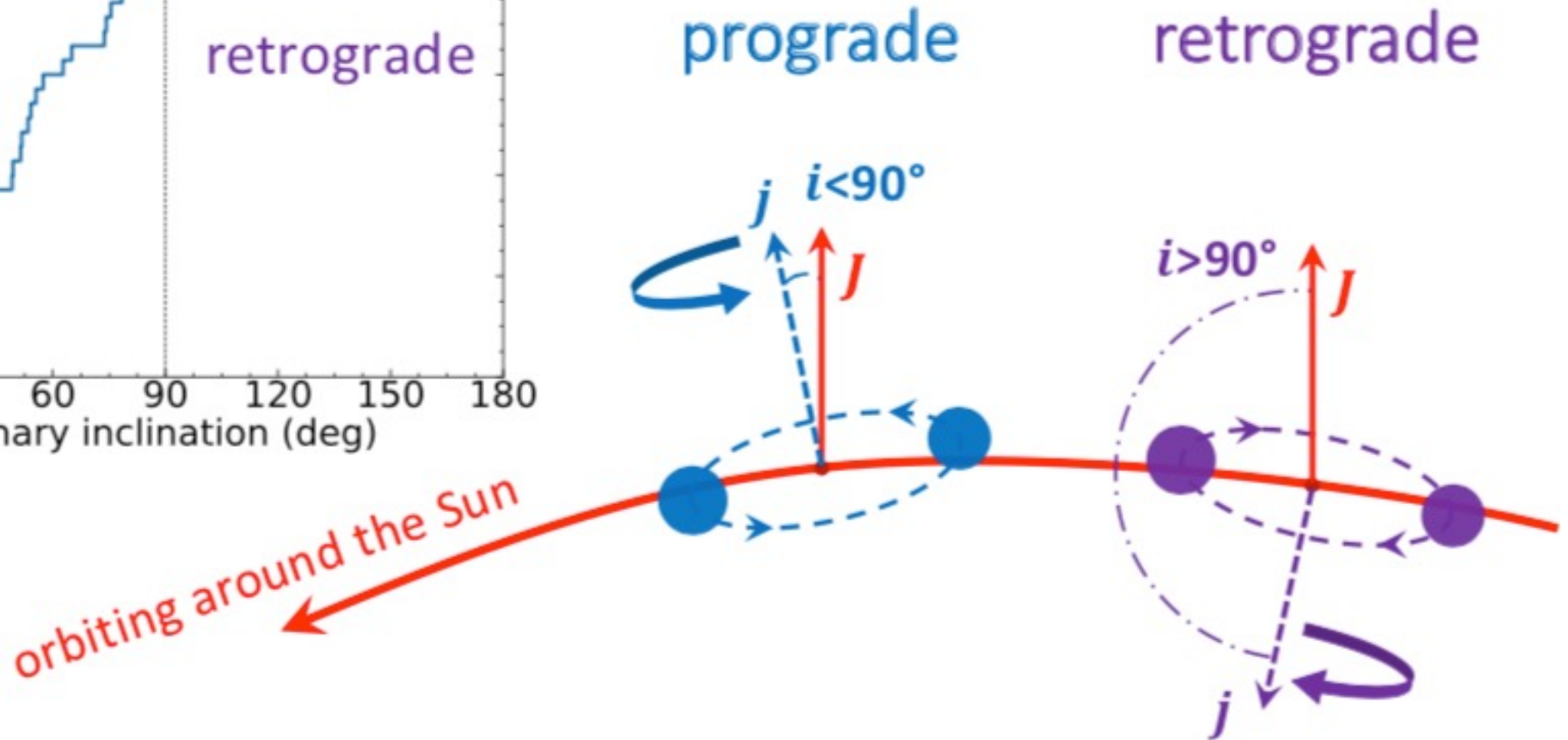
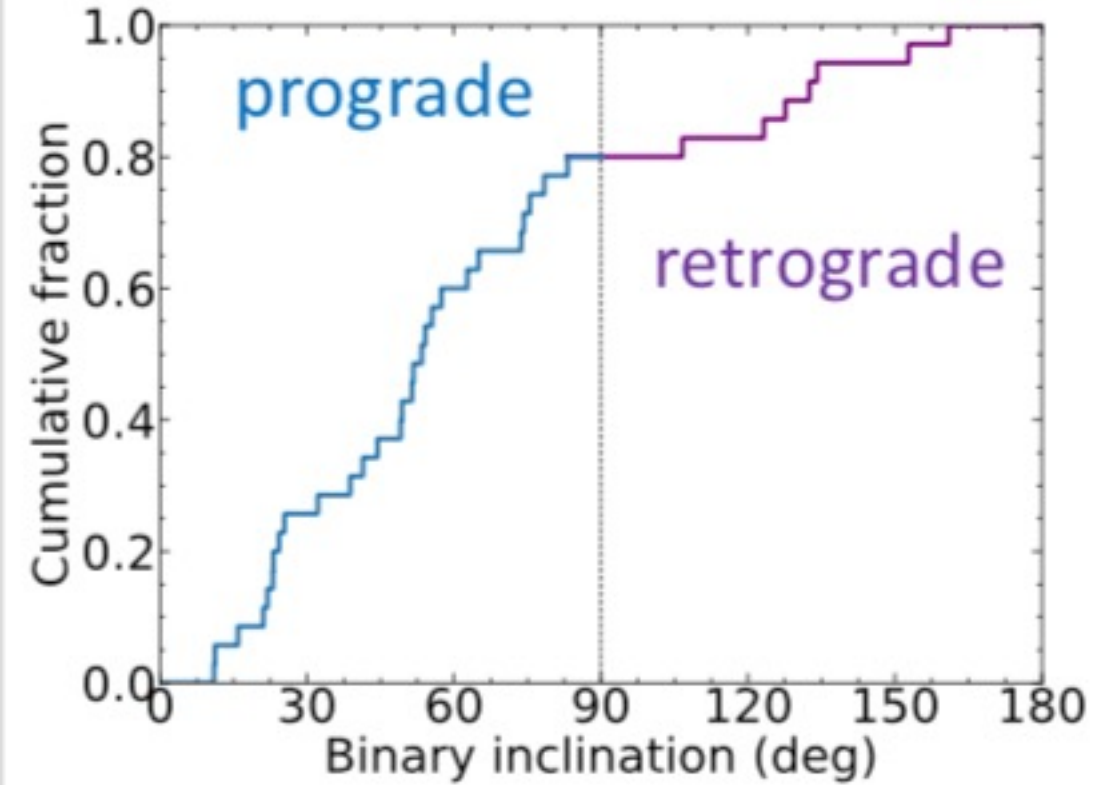


Arrokoth (MU₆₉)

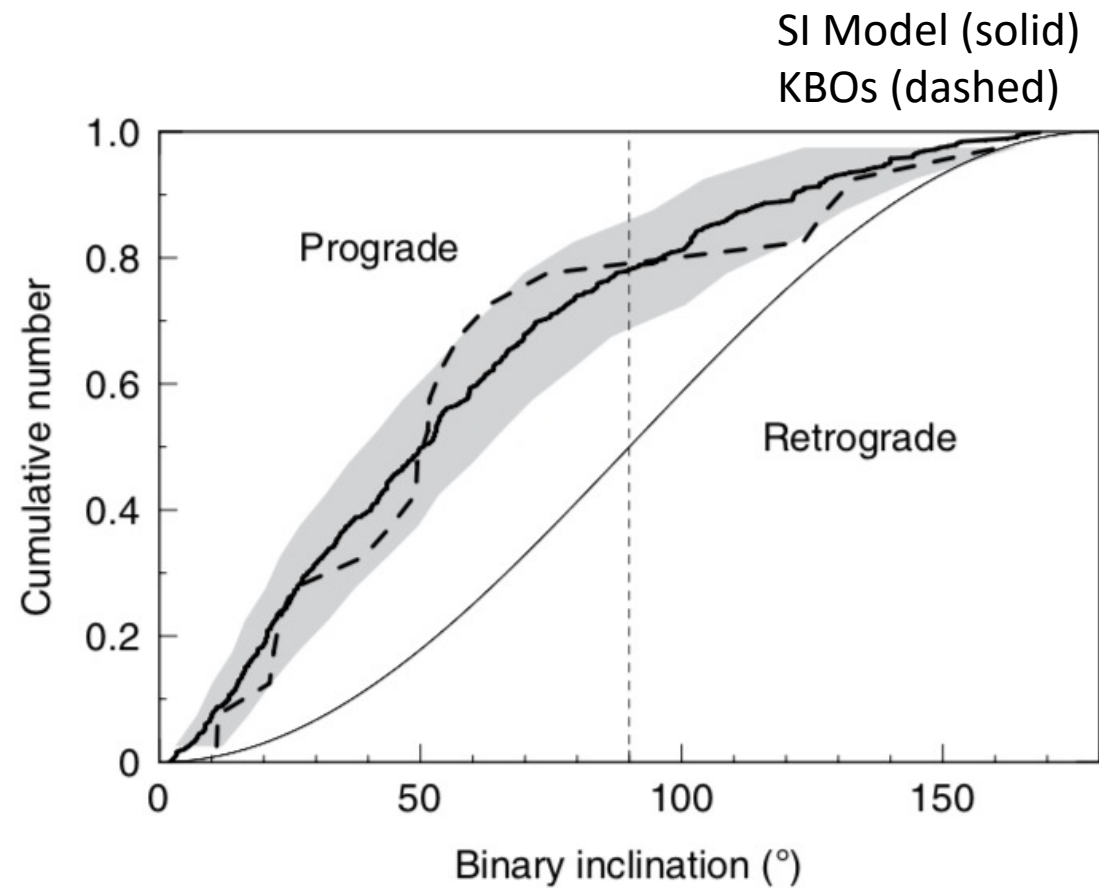
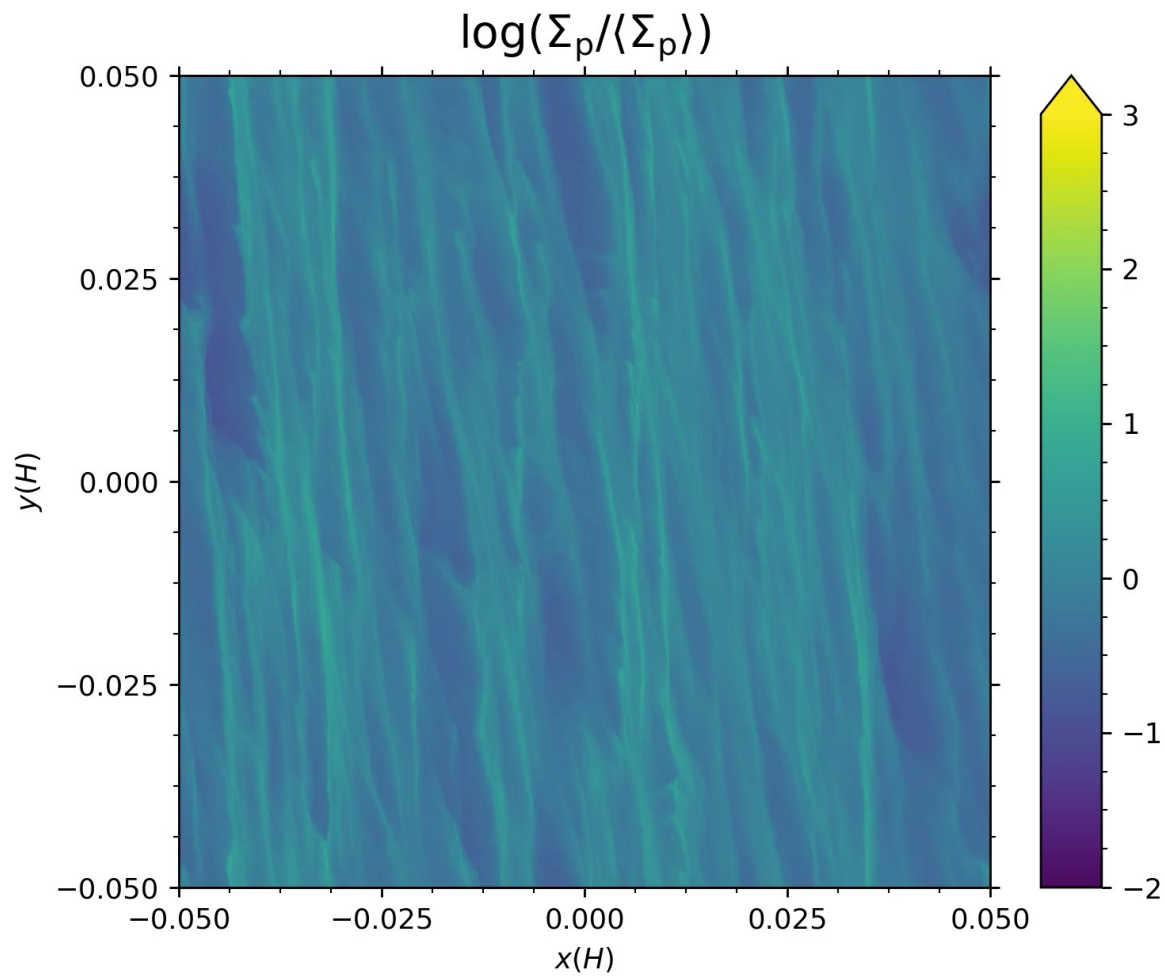


New Horizons Flyby, Jan 2019

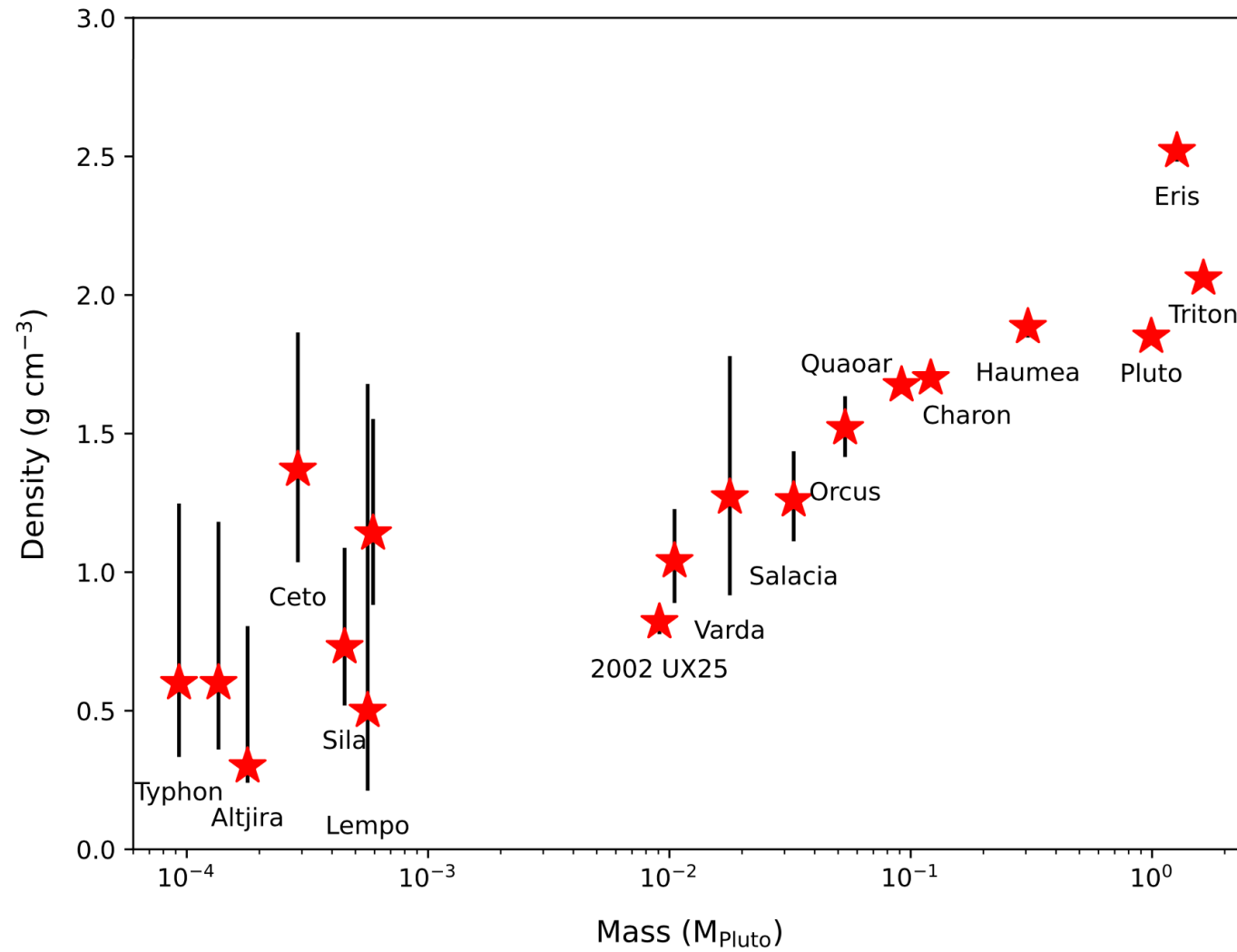
Classical KBOs: Preference for Prograde



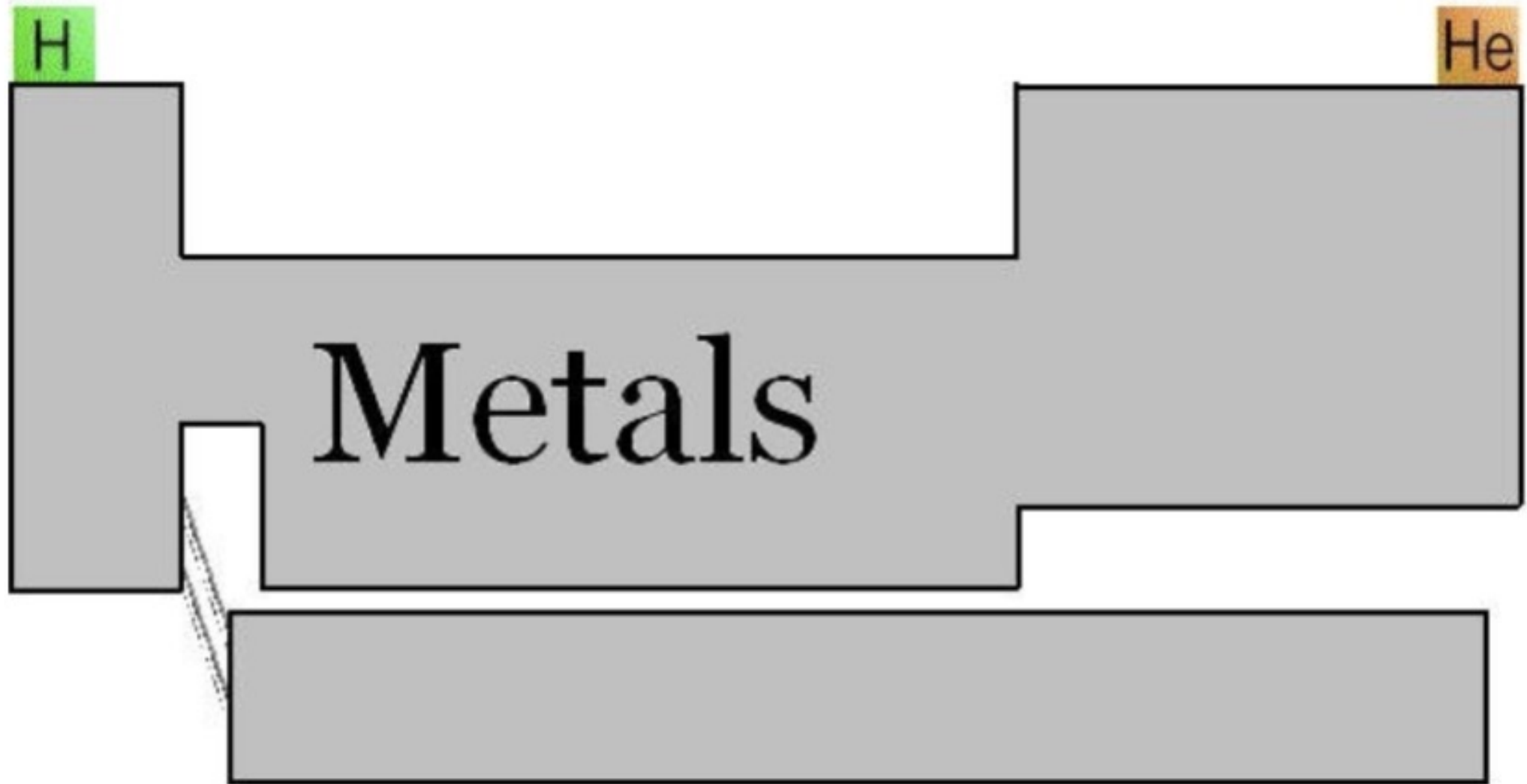
Counting binaries: Preference for Prograde (~80%)



The density dichotomy of Kuiper Belt objects

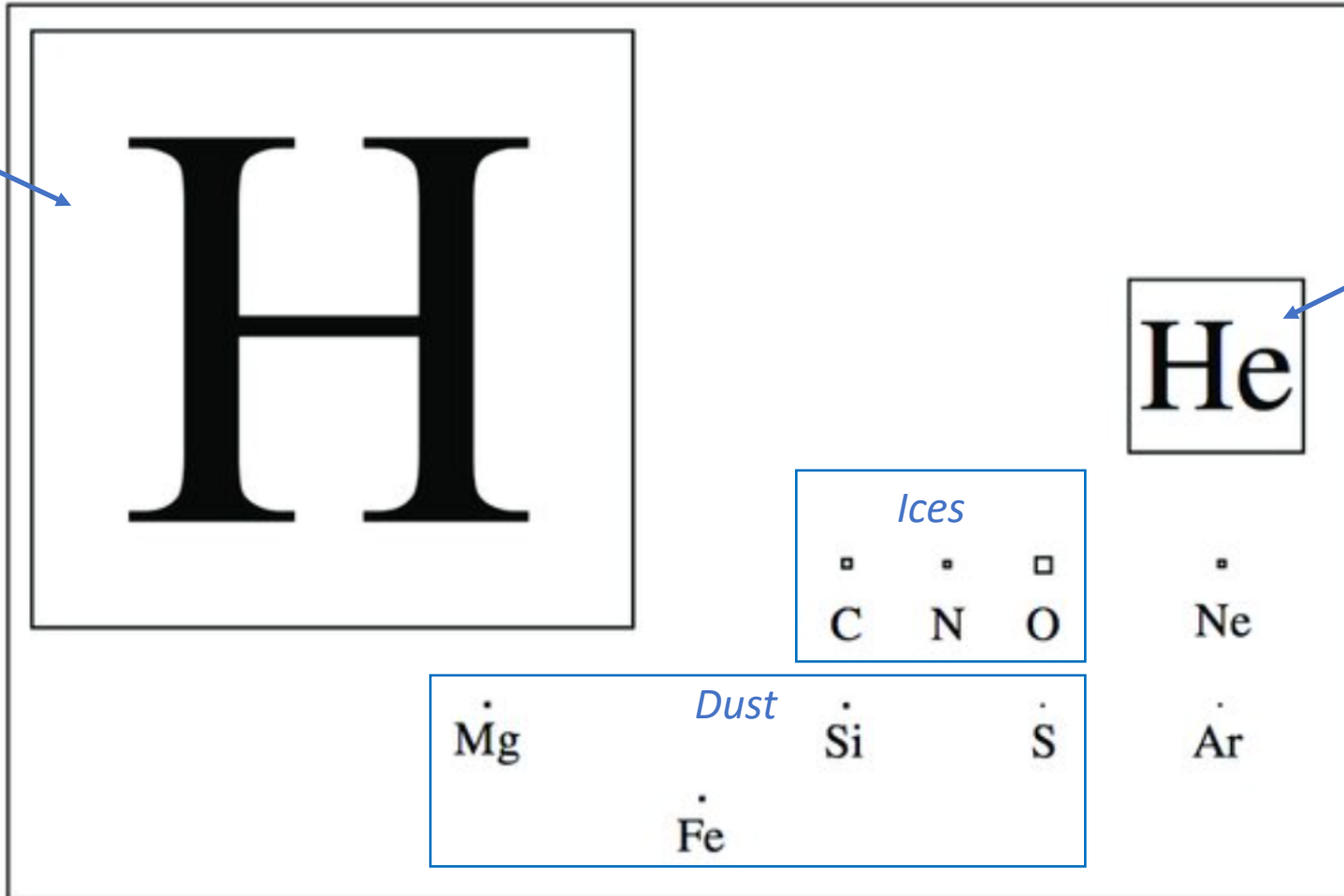


The Astronomer's Periodic Table



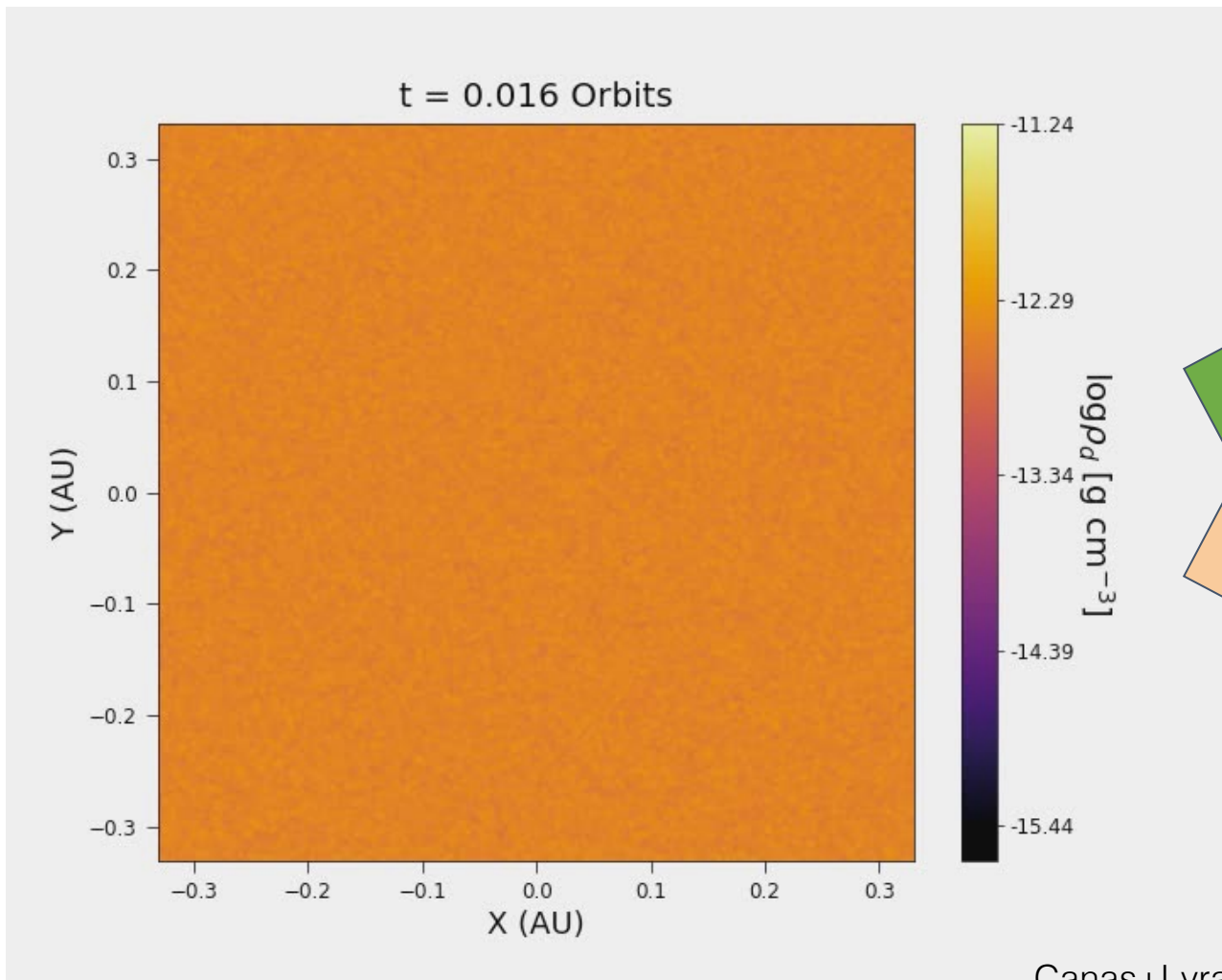
The Astronomer's Periodic Table

*Nearly everything
in the Universe*

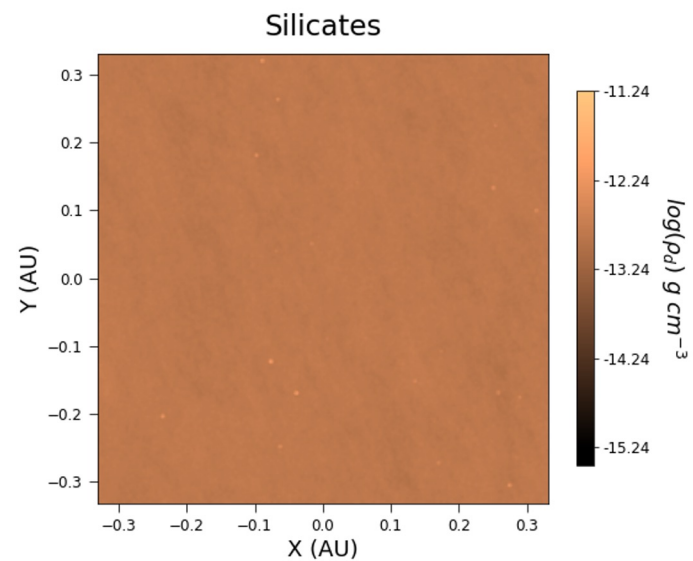
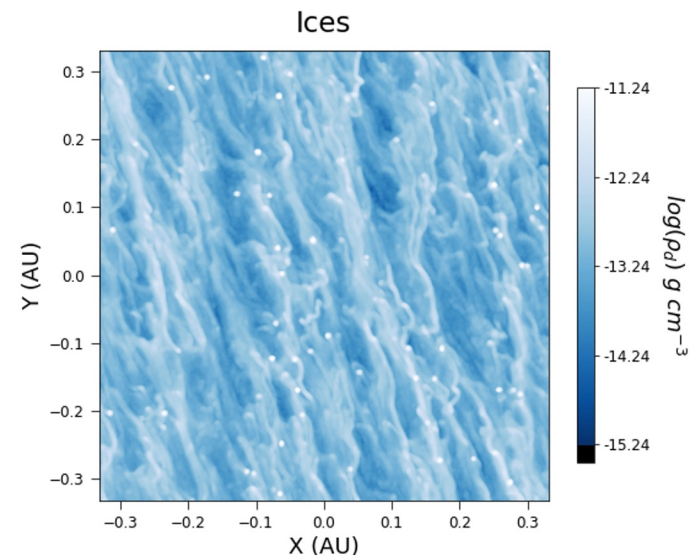


Everything else

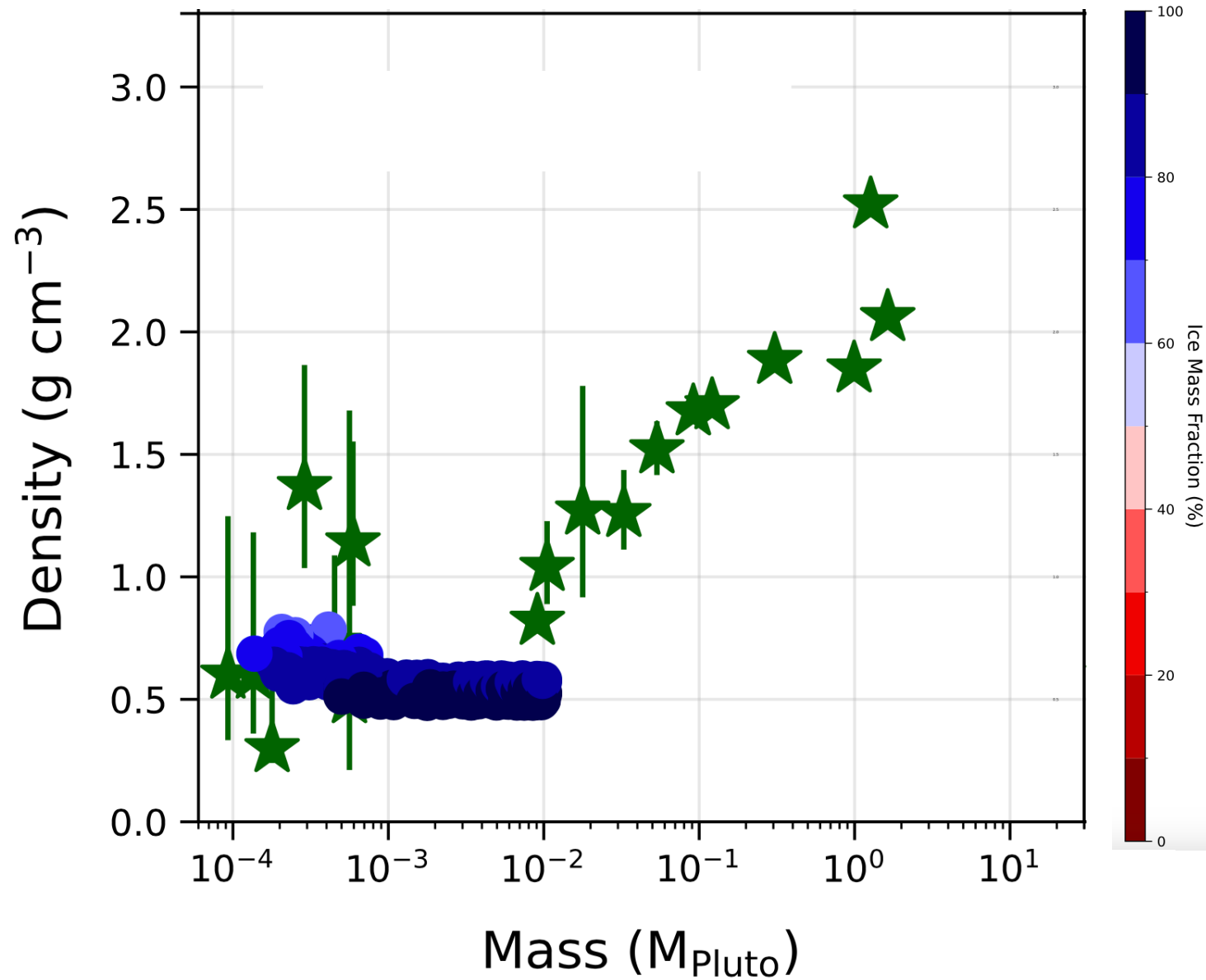
Split into icy and silicate pebbles



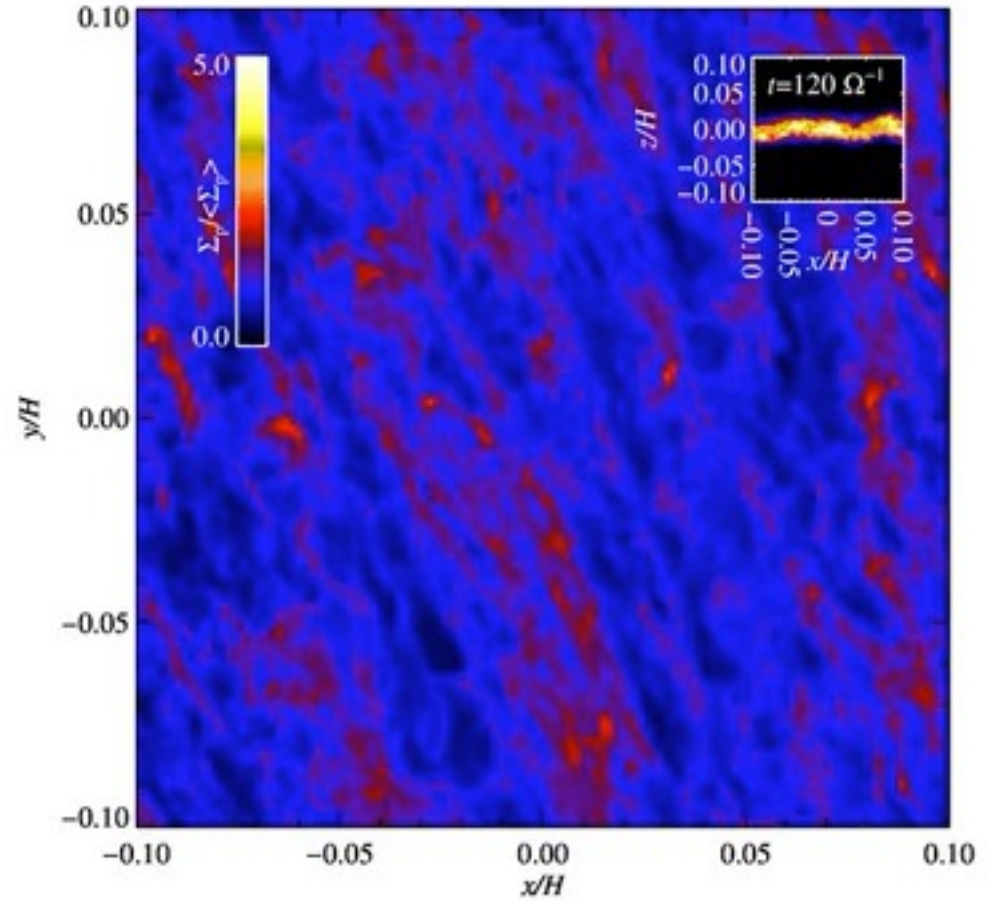
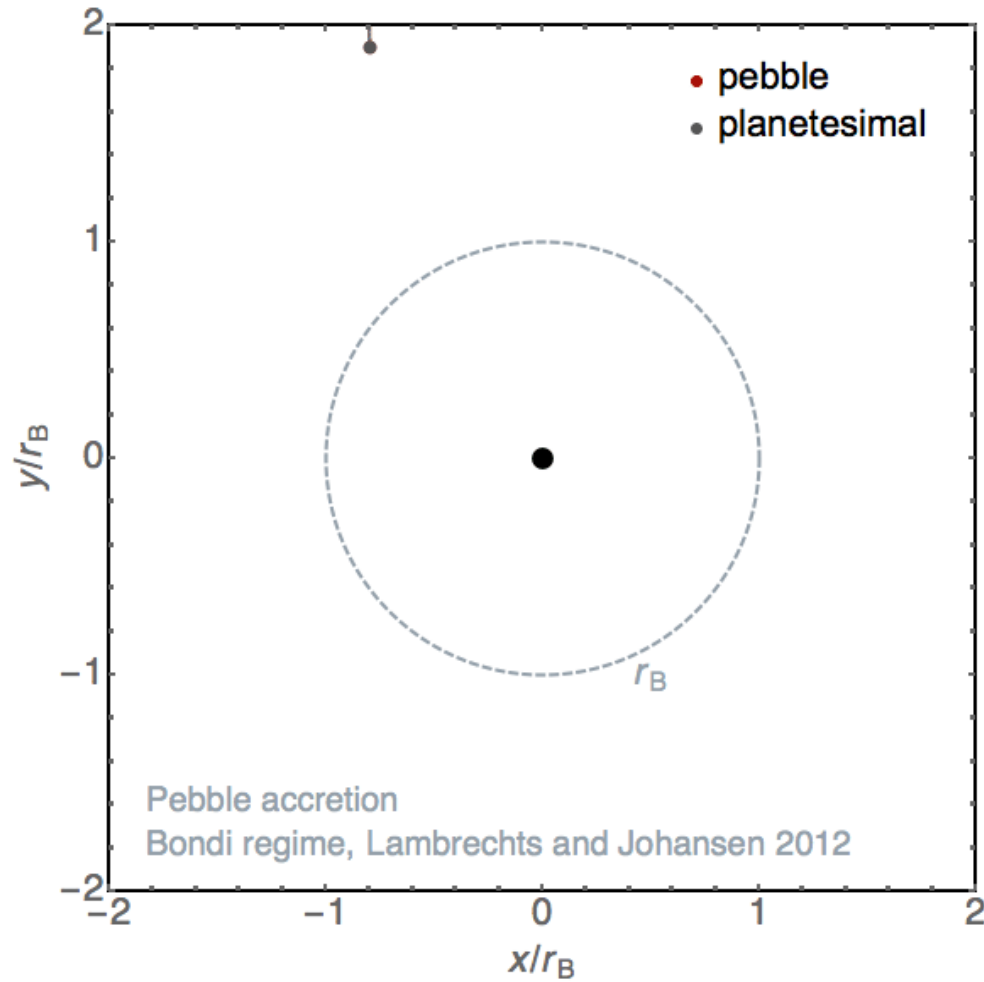
Canas+Lyra et al. 2024



The first planetesimals are icy

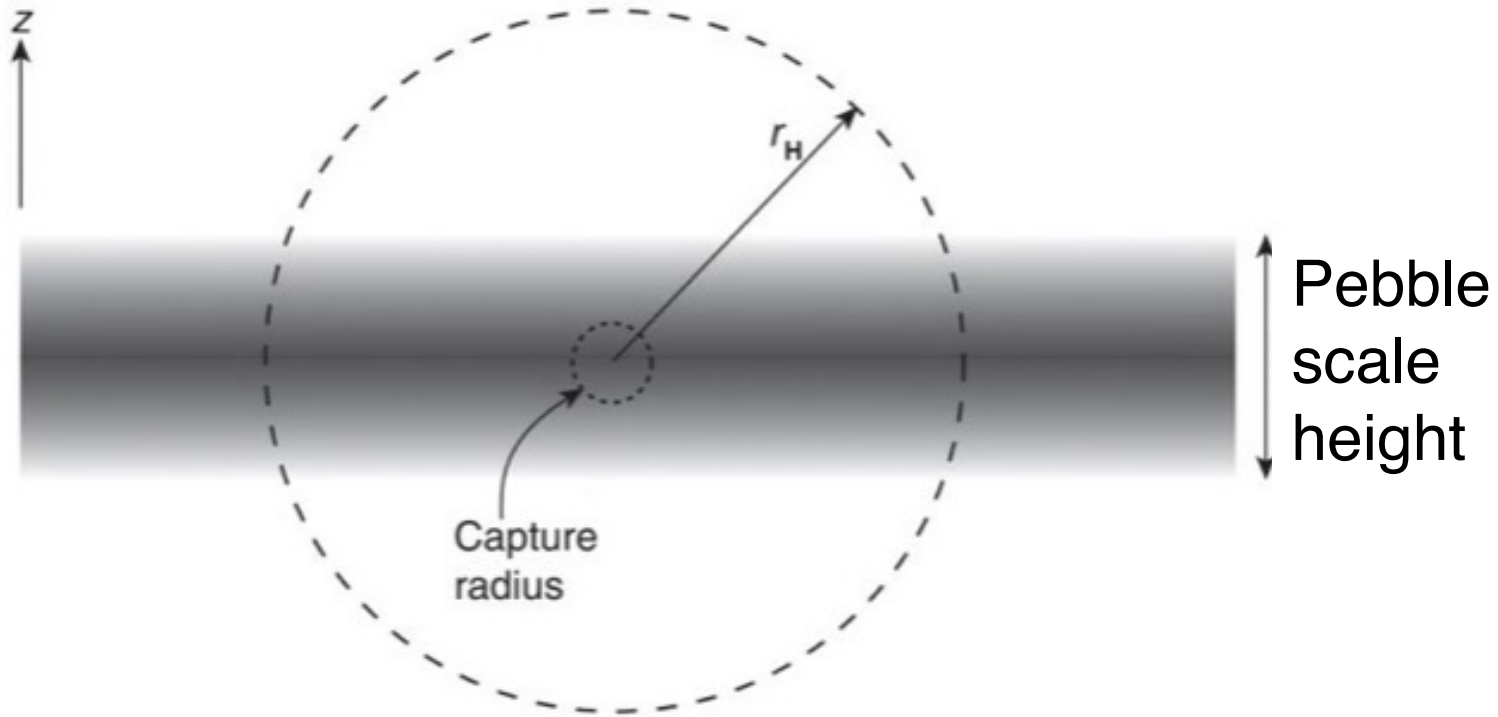


Pebble Accretion

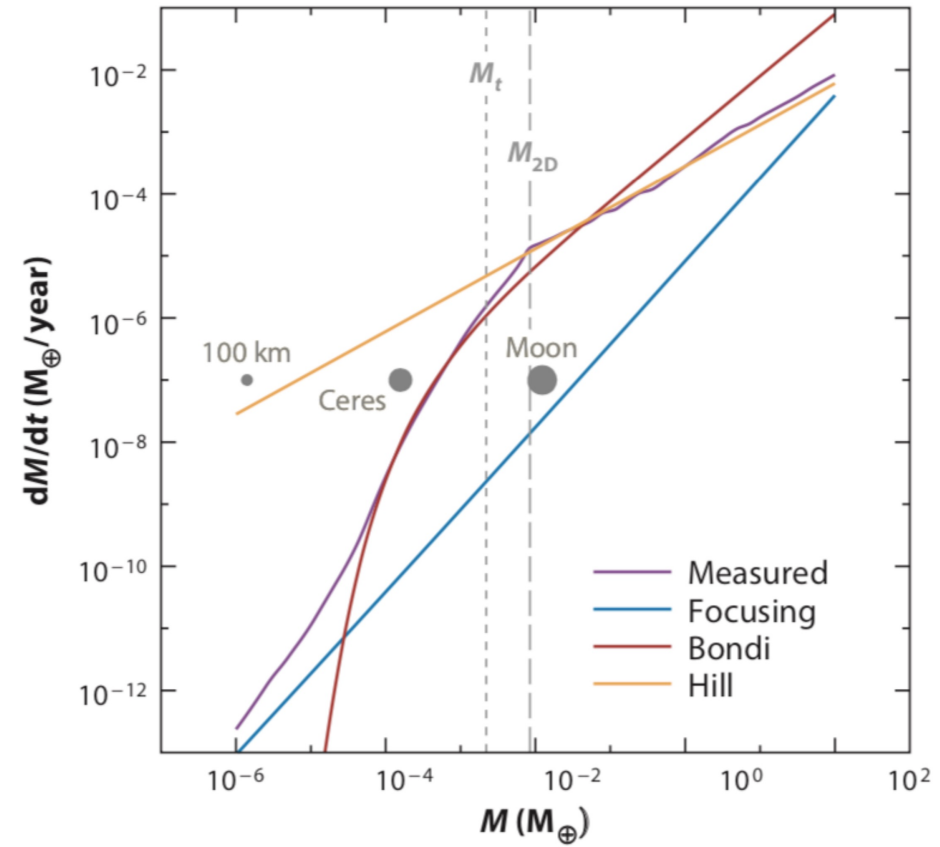


Lyra+ '08, '09, '23, Ormel & Klahr '10, Lambrechts & Johansen '12
See Johansen & Lambrechts '17 for a review

Pebble Accretion: Bondi regime and Hill regime

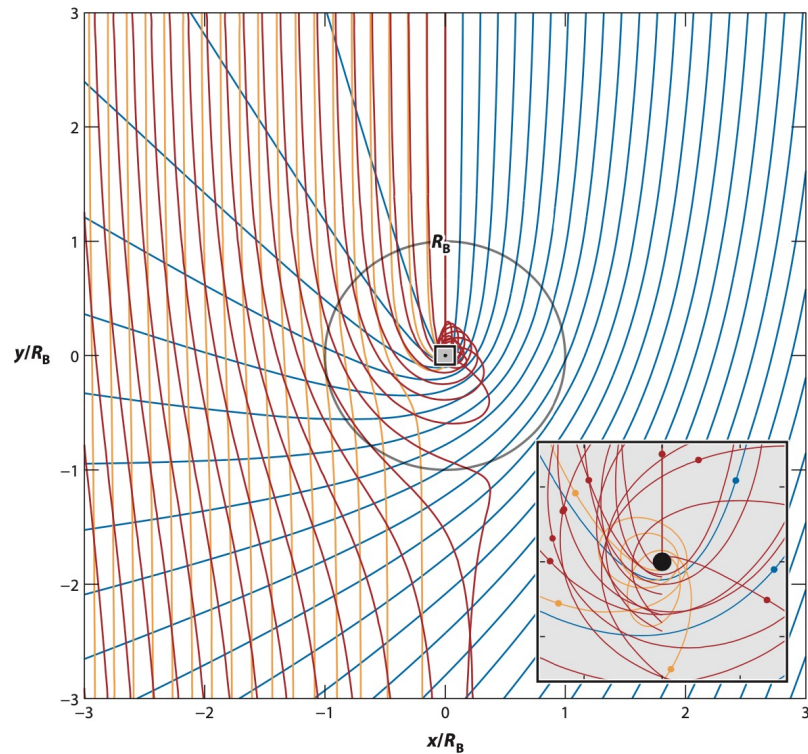


Mass Accretion rates



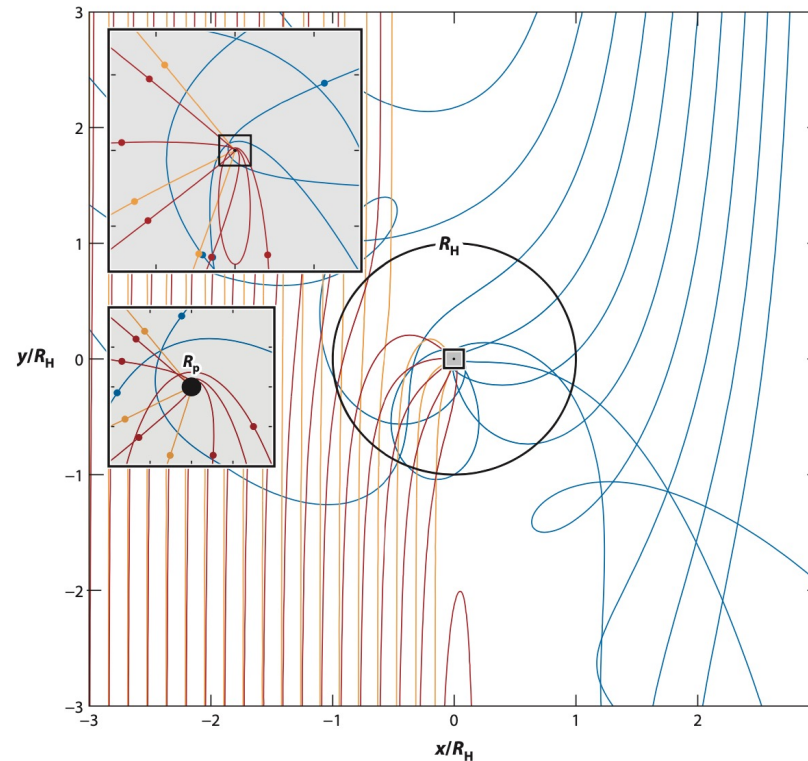
Pebble Accretion: Bondi regime and Hill regime

Bondi Regime



Best accreted
Drag time = Bondi Time

Hill Regime



Best accreted
Drag time \sim Orbital Time

Analytical theory of polydisperse (multi-species) pebble accretion

Monodisperse (single species)

$$\dot{M}_{3D} = \lim_{\xi \rightarrow 0} \dot{M} = \pi R_{\text{acc}}^2 \rho_{d0} \delta v,$$

$$\dot{M}_{2D} = \lim_{\xi \rightarrow \infty} \dot{M} = 2R_{\text{acc}} \Sigma_d \delta v,$$

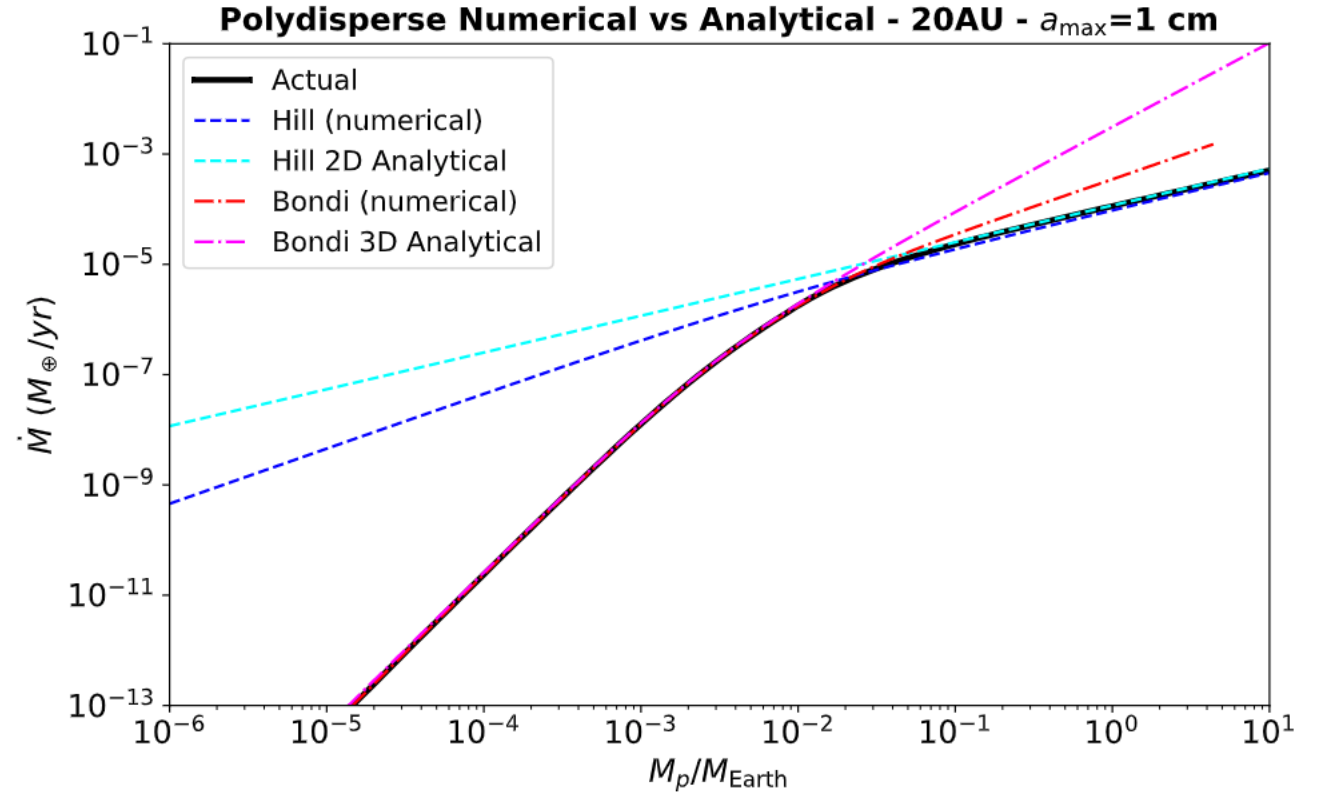
Lambrechts & Johansen (2012)

Polydisperse (multiple species)

$$\dot{M}_{2D,\text{Hill}} = \frac{6(1-p)}{14-5q-3k} \left(\frac{\text{St}_{\text{max}}}{0.1} \right)^{2/3} \Omega R_H^2 Z \Sigma_g.$$

$$\dot{M}_{3D,\text{Bondi}} \approx C_1 \frac{\gamma_l \left(\frac{b_1+1}{s}, j_1 a_{\text{max}}^s \right)}{s J_1^{(b_1+1)/s}} + C_2 \frac{\gamma_l \left(\frac{b_2+1}{s}, j_2 a_{\text{max}}^s \right)}{s J_2^{(b_2+1)/s}} + C_3 \frac{\gamma_l \left(\frac{b_3+1}{s}, j_3 a_{\text{max}}^s \right)}{s J_3^{(b_3+1)/s}} + C_4 \frac{\gamma_l \left(\frac{b_4+1}{s}, j_4 a_{\text{max}}^s \right)}{s J_4^{(b_4+1)/s}},$$

Lyra et al. (2023)



Lyra et al. 2023

Bondi (Low-Mass regime) is 1-2 orders of magnitude more efficient than monodisperse

Monodisperse (single species)

$$\dot{M}_{3D} = \lim_{\xi \rightarrow 0} \dot{M} = \pi R_{\text{acc}}^2 \rho_{d0} \delta v,$$

$$\dot{M}_{2D} = \lim_{\xi \rightarrow \infty} \dot{M} = 2R_{\text{acc}} \Sigma_d \delta v,$$

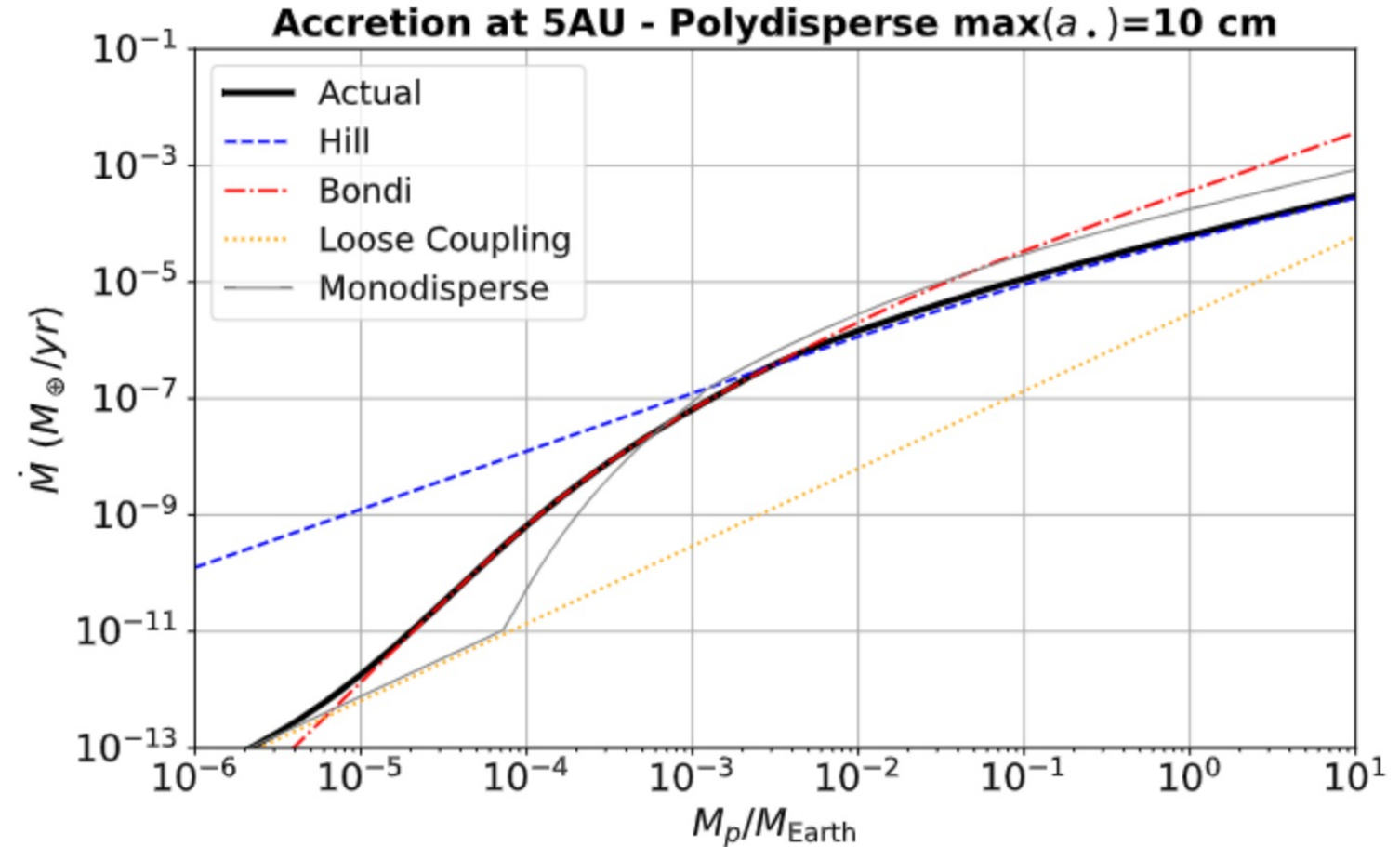
Lambrechts & Johansen (2012)

Polydisperse (multiple species)

$$\dot{M}_{2D,\text{Hill}} = \frac{6(1-p)}{14-5q-3k} \left(\frac{\text{St}_{\text{max}}}{0.1} \right)^{2/3} \Omega R_H^2 Z \Sigma_g.$$

$$\dot{M}_{3D,\text{Bondi}} \approx C_1 \frac{\gamma_l \left(\frac{b_1+1}{s}, j_1 a_{\text{max}}^s \right)}{s j_1^{(b_1+1)/s}} + C_2 \frac{\gamma_l \left(\frac{b_2+1}{s}, j_2 a_{\text{max}}^s \right)}{s j_2^{(b_2+1)/s}} + C_3 \frac{\gamma_l \left(\frac{b_3+1}{s}, j_3 a_{\text{max}}^s \right)}{s j_3^{(b_3+1)/s}} + C_4 \frac{\gamma_l \left(\frac{b_4+1}{s}, j_4 a_{\text{max}}^s \right)}{s j_4^{(b_4+1)/s}},$$

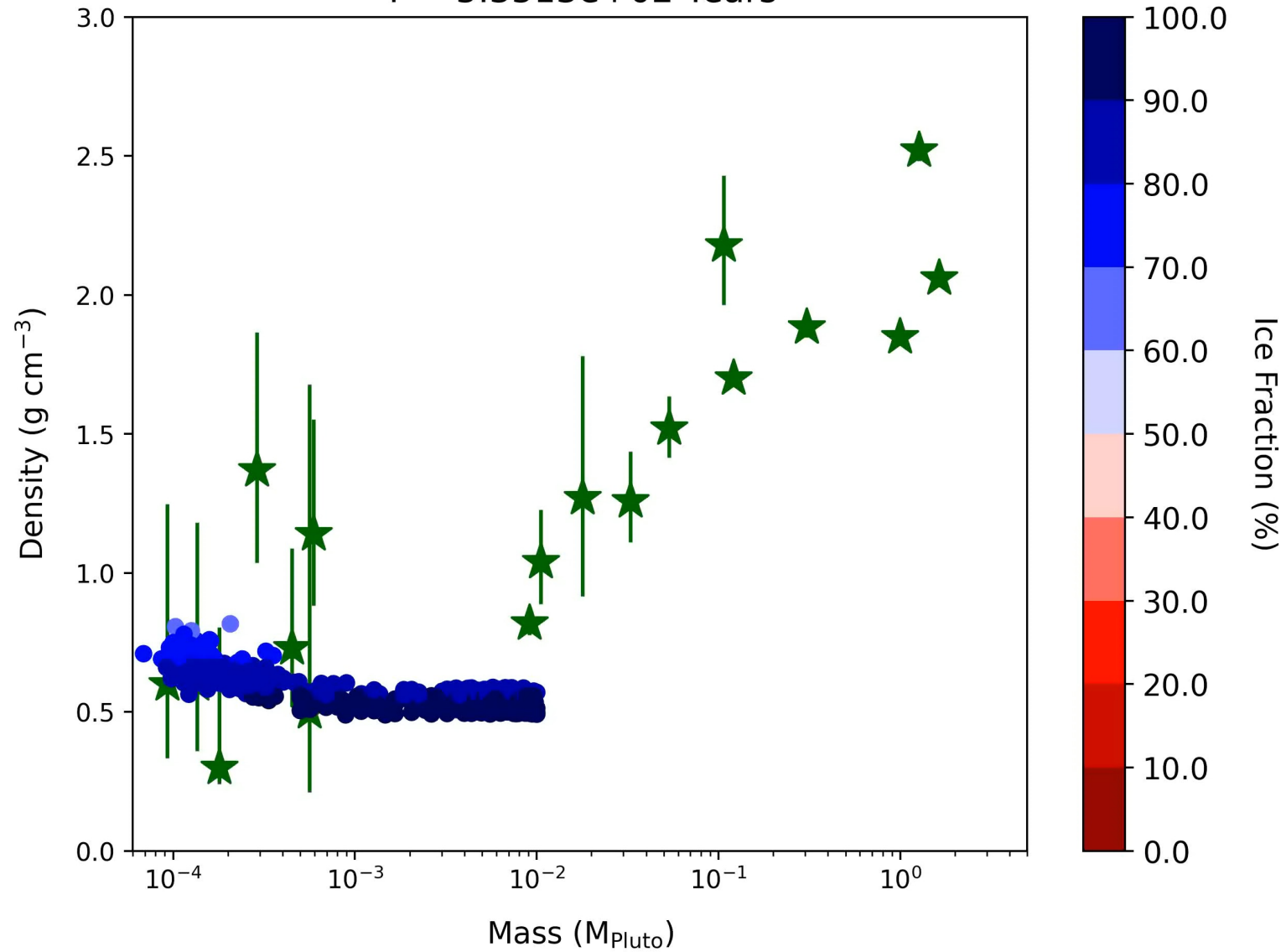
Lyra et al. (2023)



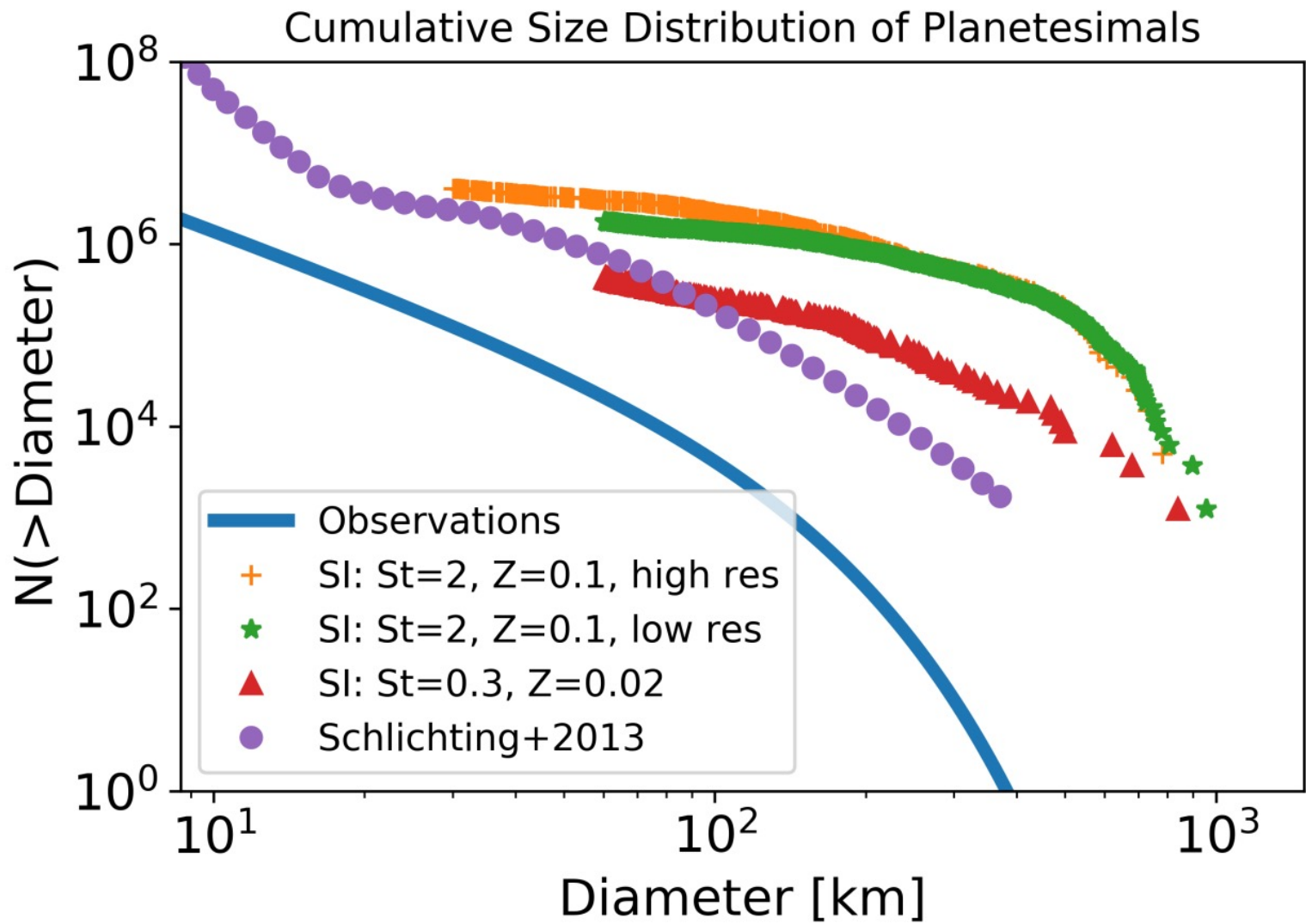
Lyra et al. 2023

Growing Pluto by silicate pebble accretion

T = 5.3513e+02 Years



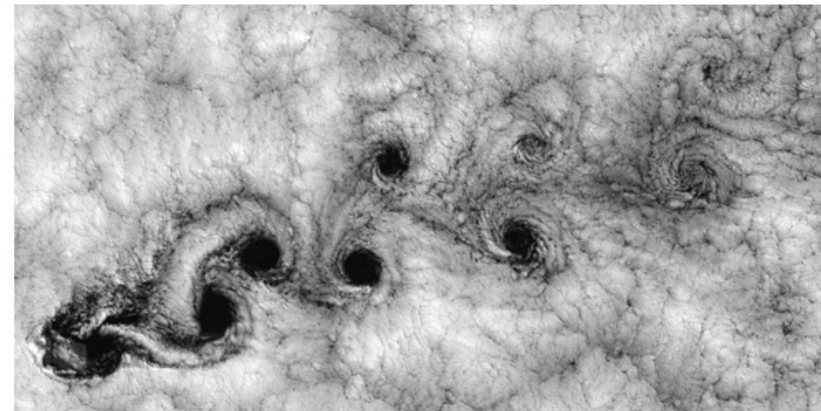
Problem: wrong number density



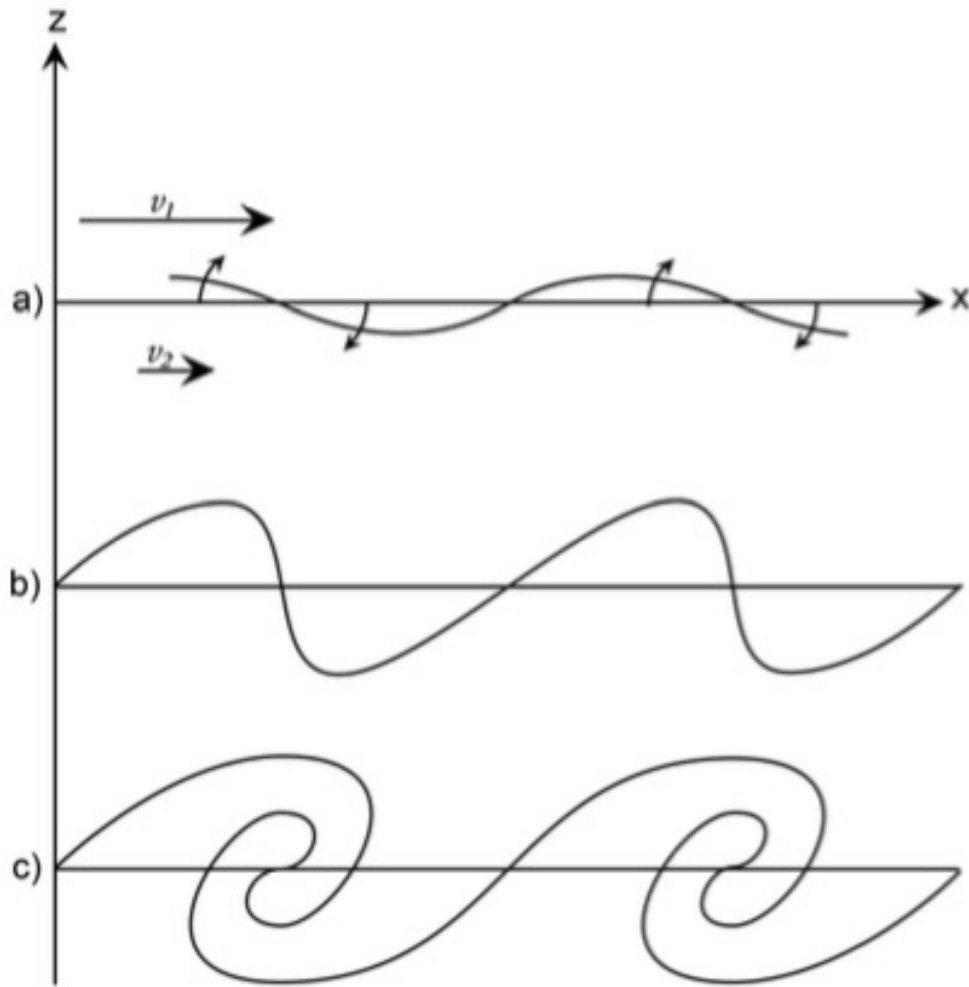
Vortices – an ubiquitous fluid mechanics phenomenon



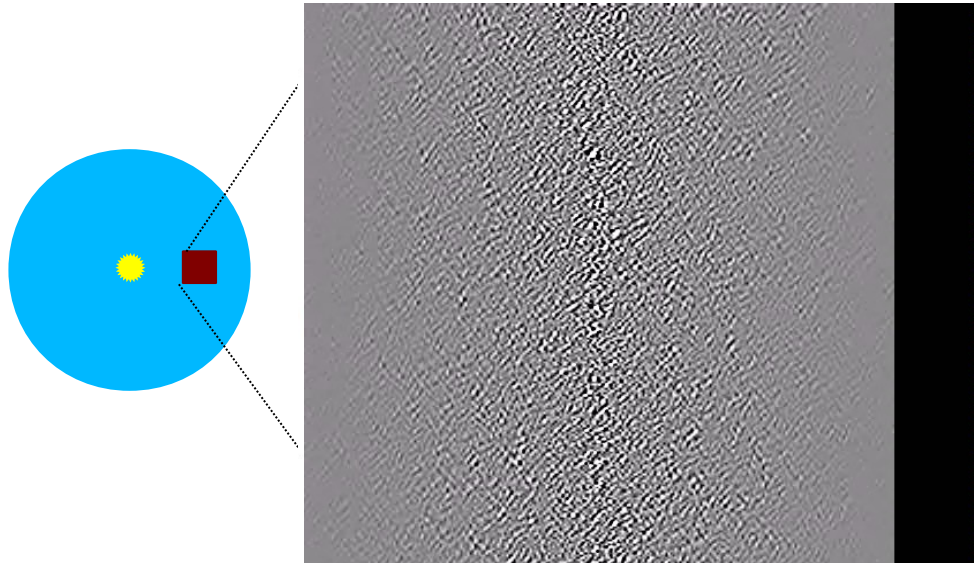
Von Kármán vortex street



Kelvin-Helmholtz Instability

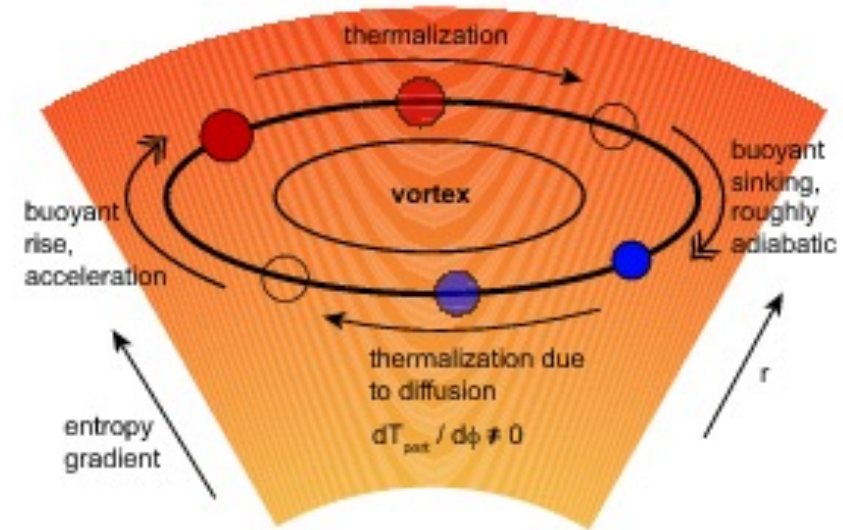


Convection



Lyra & Klahr (2011)
Klahr & Hubbard (2014)
Lyra (2014)
Latter (2016)
Volponi (2016)
Reed & Latter (2021)
Raettig et al. (2021)

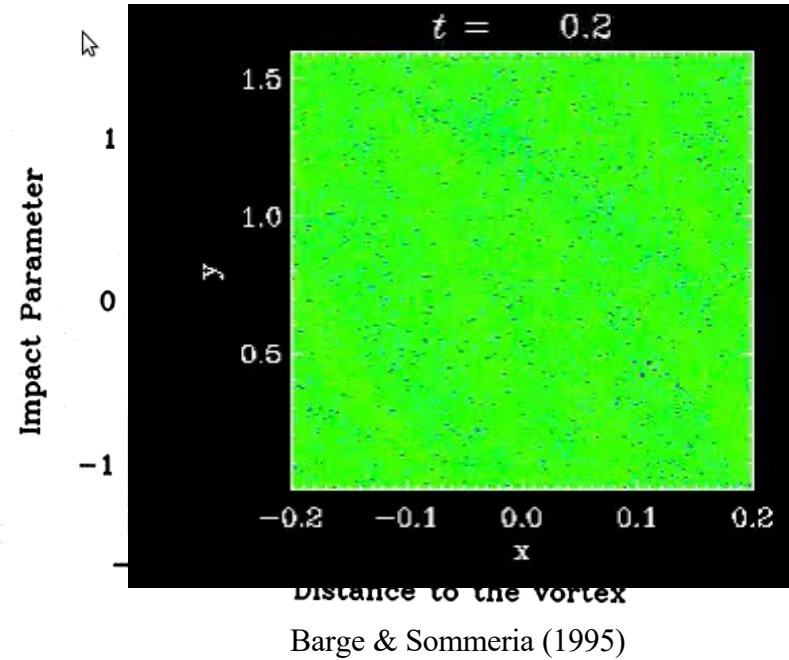
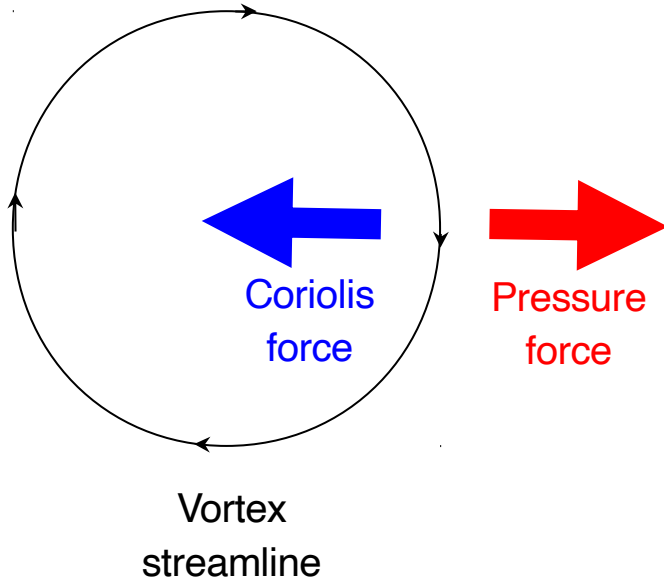
Sketch of the Convective Instability



Armitage (2010)

Vortex Trapping

Geostrophic balance:



Grains do not feel the pressure gradient.
They sink towards the center, where they accumulate.

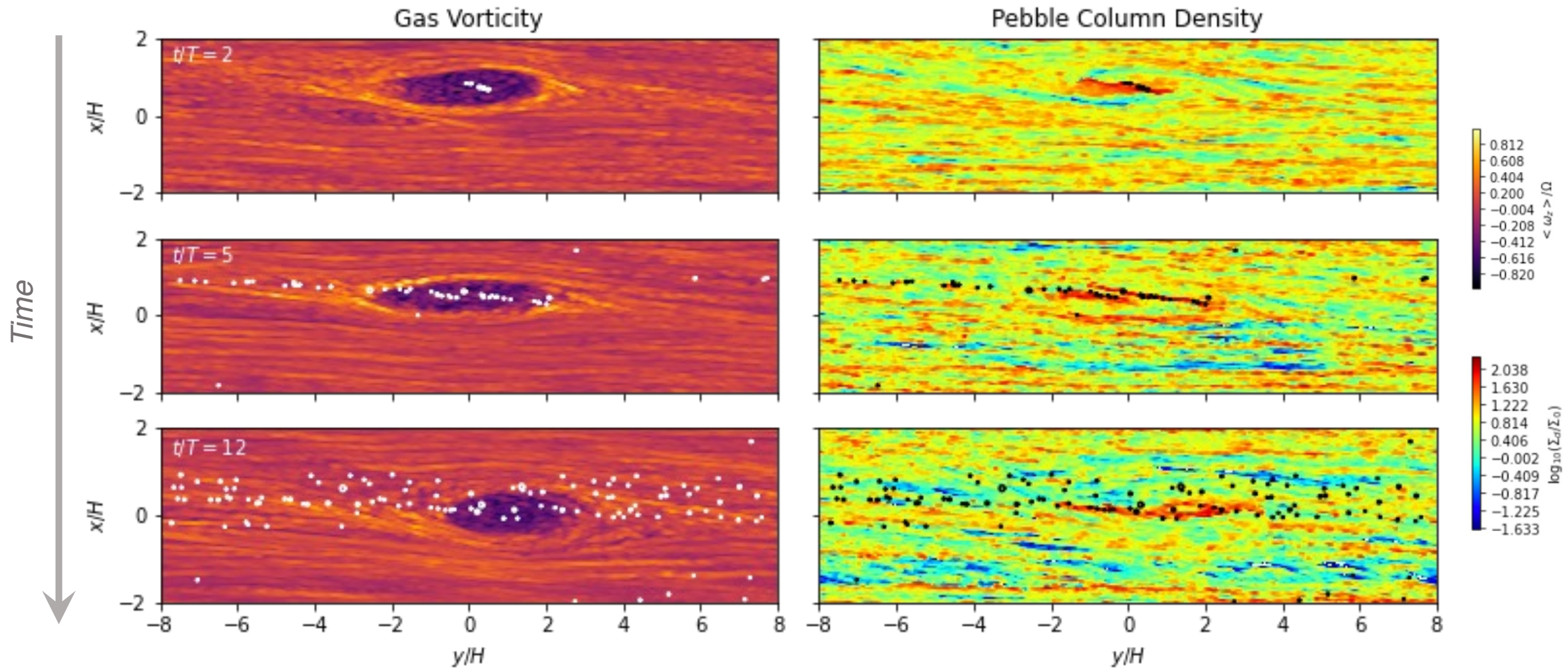
Aid to planet formation

(Barge & Sommeria 1995, Tanga et al. 1996, Adams et al. 1996)

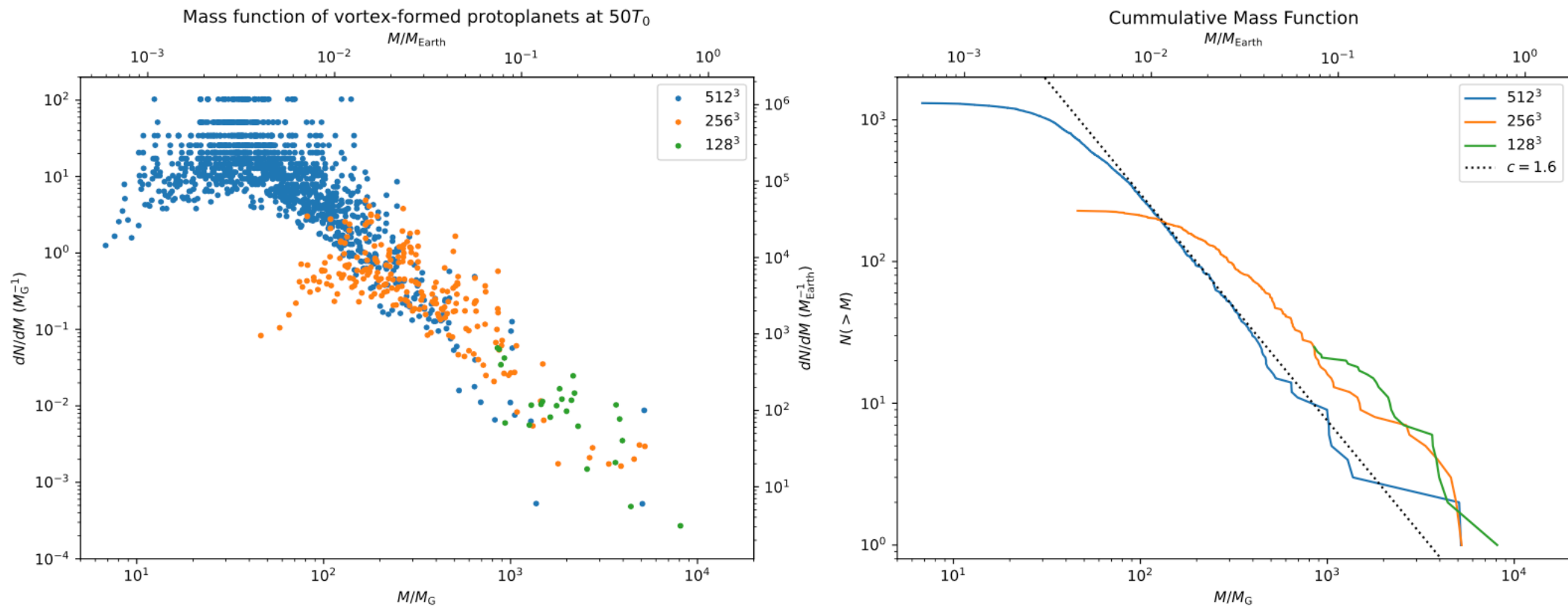
Speeds up planet formation enormously

(Lyra et al. 2008b, 2009ab, Raettig et al. 2012, 2021)

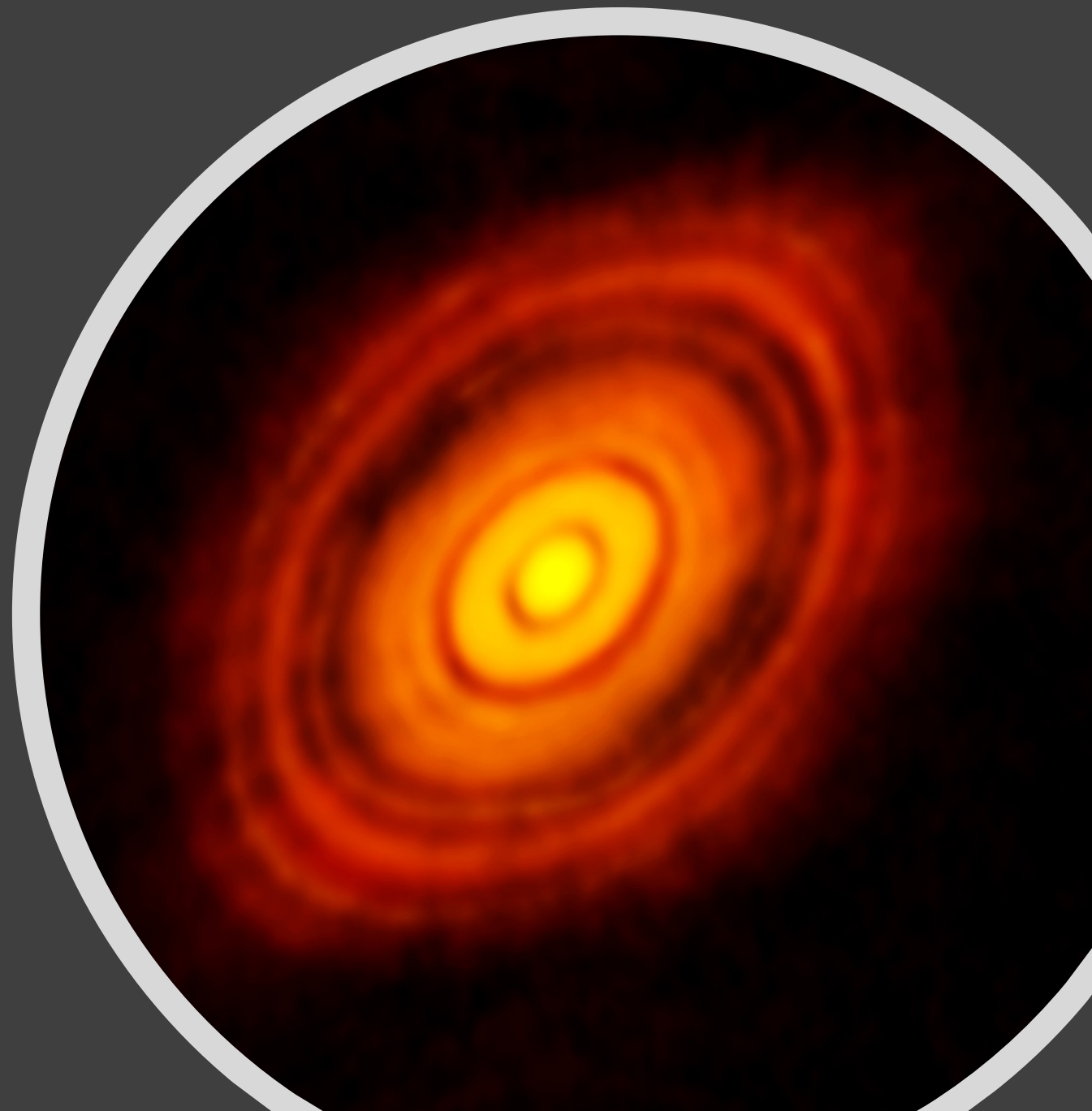
Vortex Trapping



Vortex Trapping – Initial Mass Function



Disk
Observations



Transits

A diagram illustrating the transit method. On the left, a telescope on a tripod is shown. To its right is a graph showing a light curve with a characteristic dip. On the right, a star (yellow star) is shown with a green planet orbiting it, passing in front of the star.

Radial velocities

A diagram illustrating the radial velocity method. On the left, a telescope on a tripod is shown. To its right is a graph showing a light curve with a characteristic dip. On the right, a star (yellow star) is shown with a green planet orbiting it, and a blue wavy line and a red wavy line represent the Doppler shift in the star's light.

Microlensing

A diagram illustrating the gravitational microlensing method. On the left, a telescope on a tripod is shown. To its right is a graph showing a light curve with a characteristic peak. On the right, a star (yellow star) is shown with a green planet orbiting it, and a dashed line indicates the path of a distant star passing near the star-planet system.

Timing variations

A diagram illustrating the timing variations method. On the left, a telescope on a tripod is shown. To its right is a graph showing a light curve with a characteristic dip. On the right, a star (yellow star) is shown with a blue planet and a green planet orbiting it, with the blue planet's orbit being significantly tilted.

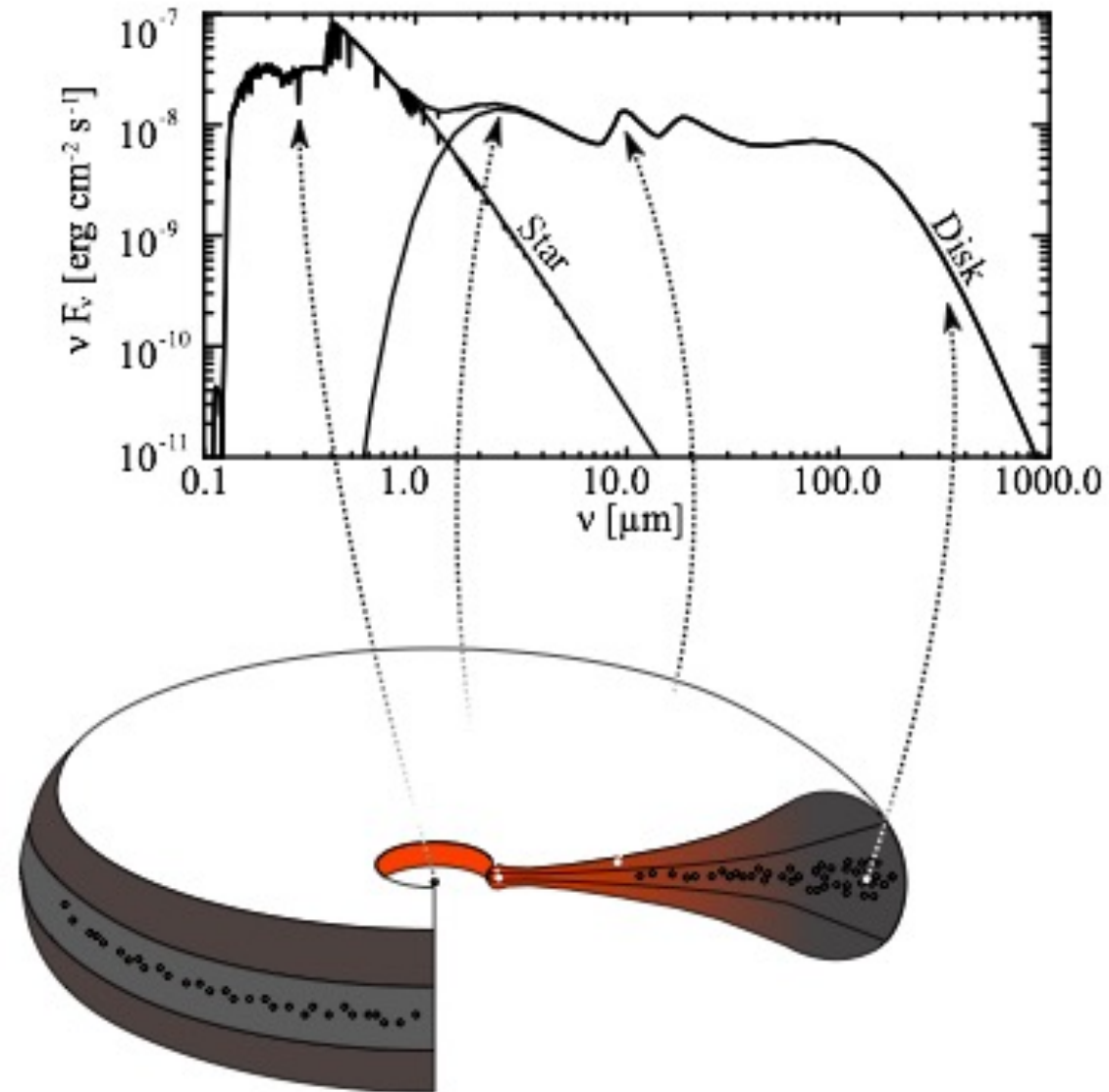
Direct imaging

A diagram illustrating the direct imaging method. On the left, a telescope on a tripod is shown. On the right, a star (yellow star) is shown with a green planet orbiting it, and the planet is shown as a distinct point of light.

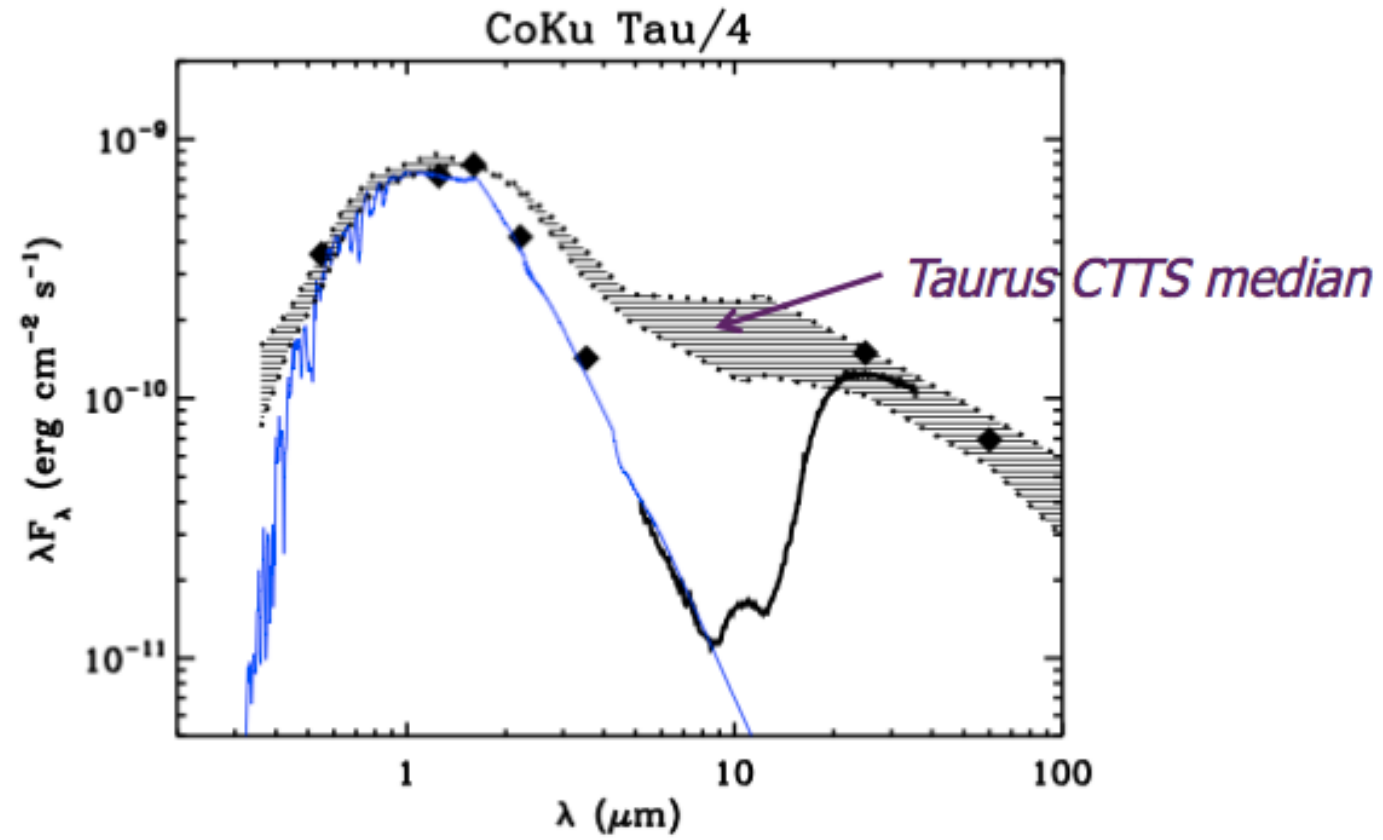
Disk interactions

A diagram illustrating the disk interactions method. On the left, a telescope on a tripod is shown. On the right, a star (yellow star) is shown with a green planet orbiting it, and a large orange and red disk is shown around the star, representing a protoplanetary disk or a debris disk.

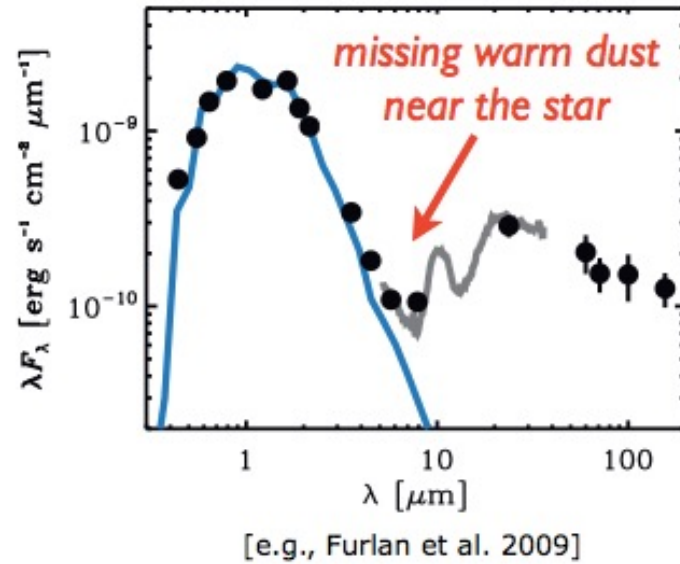
Disk spectra



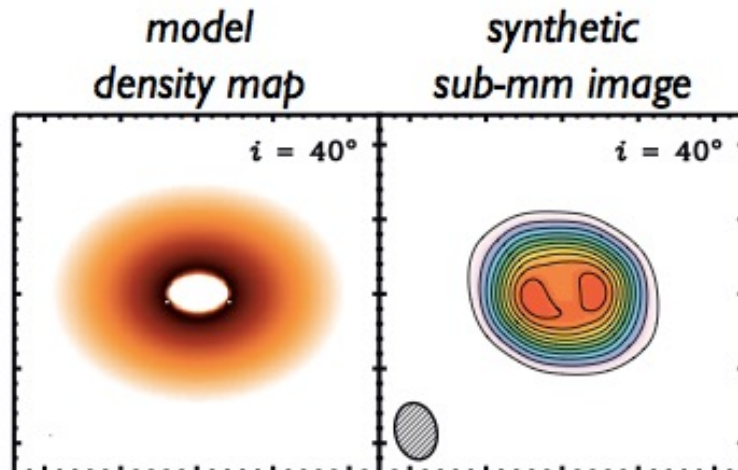
A class of disks with missing hot dust.



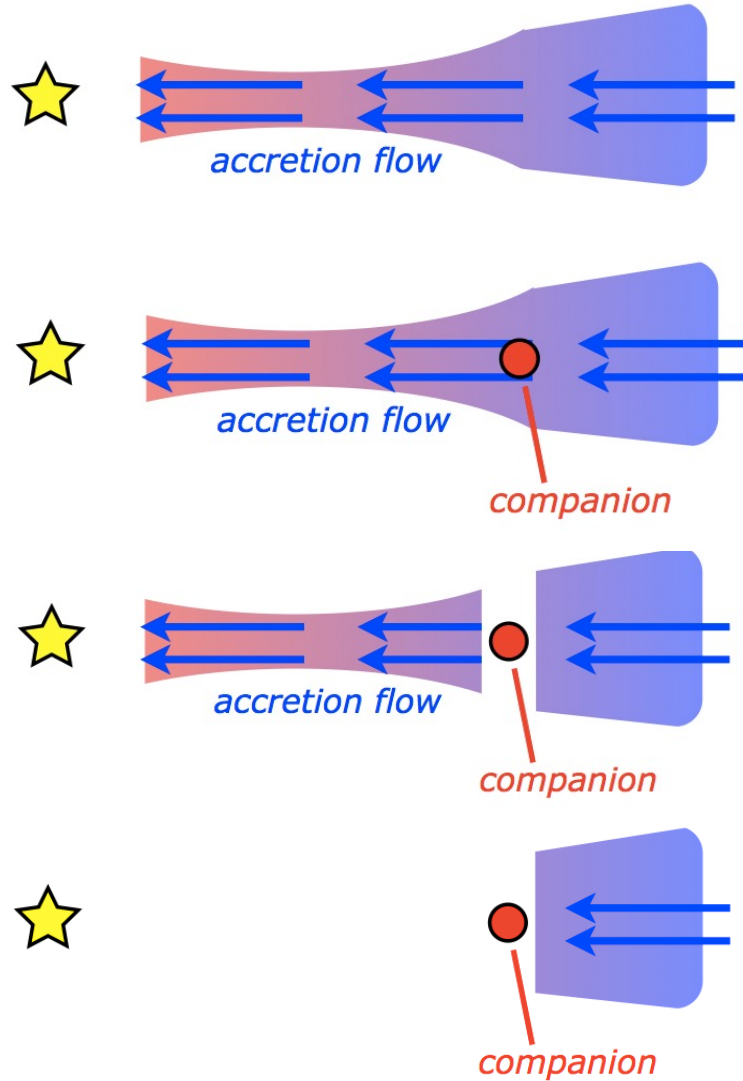
Disks with missing hot dust.



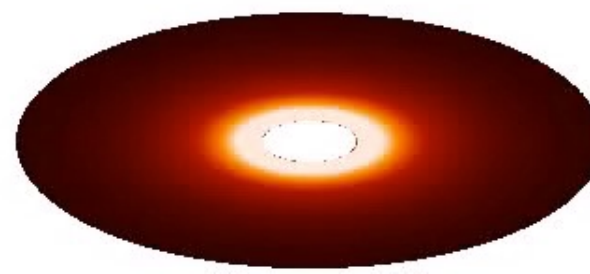
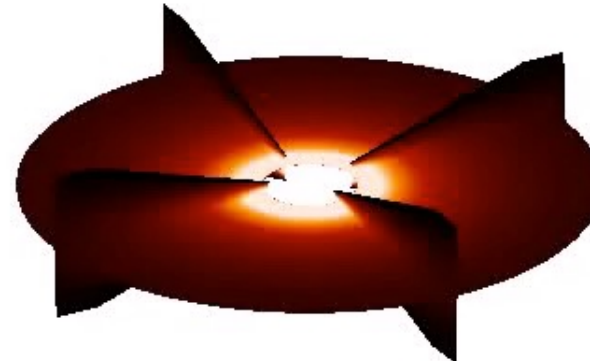
a disk with a large reduction in optical depth near the star (i.e., a "cavity" or "hole")



Planetary companion

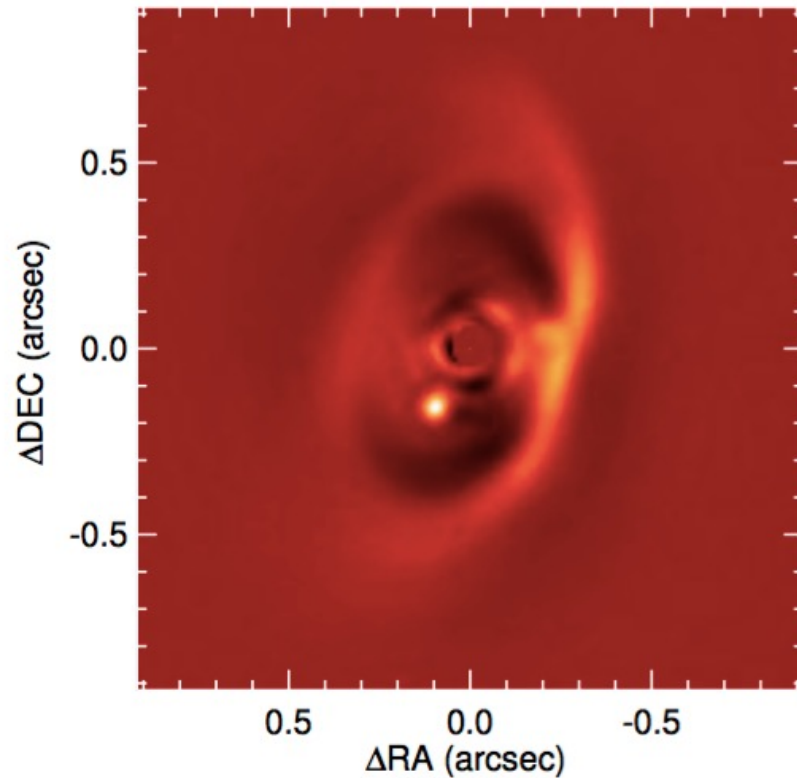


$t = 0.1$

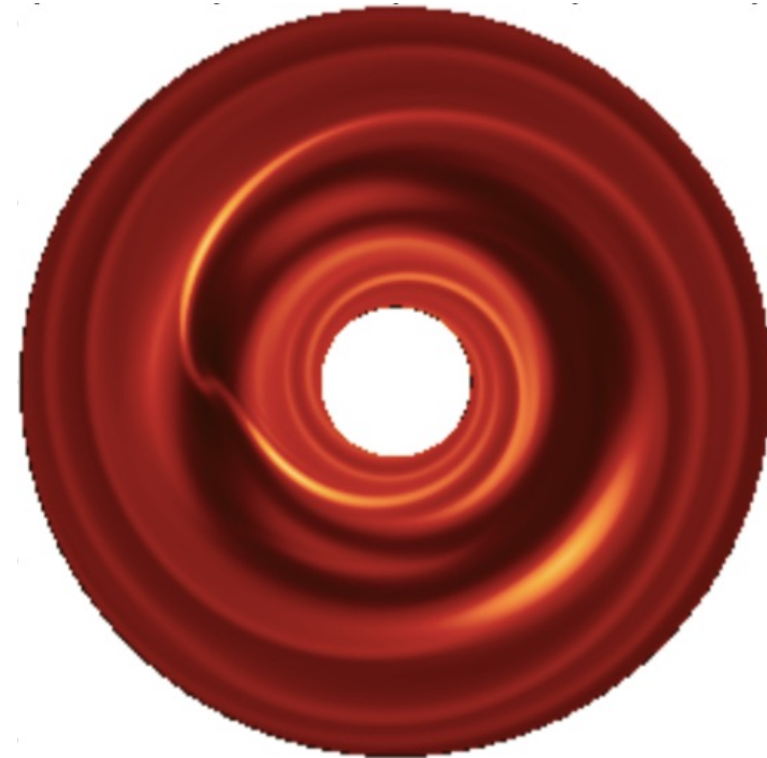


These cavities may be the telltale signature of forming planets

PDS 70 and PDS 70b



(Muller et al. 2018)



(Lyra et al. 2009b)

A way to directly study planet-disk interaction

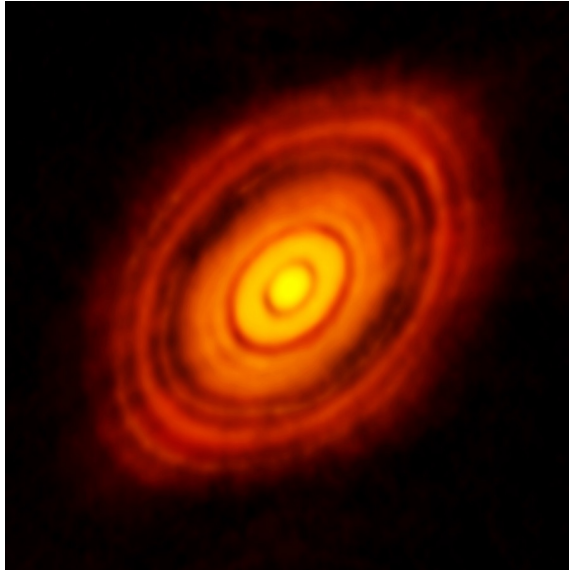
Planet-disk interaction: gaps, spirals, and vortices.



(Lyra et al. 2009b)

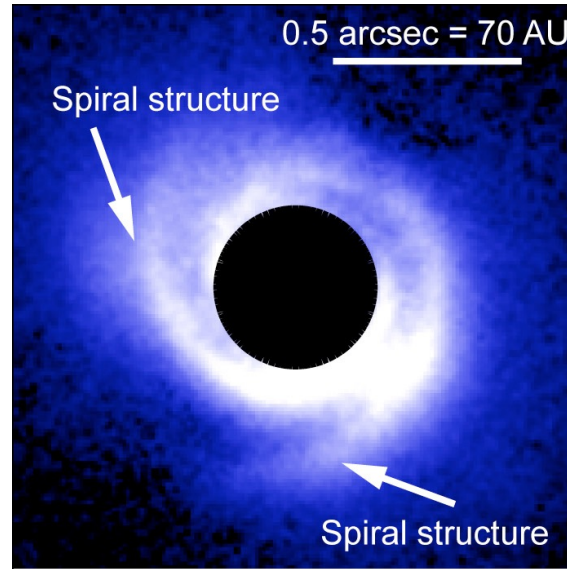
Observational evidence: gaps, spirals, and vortices

HL Tau



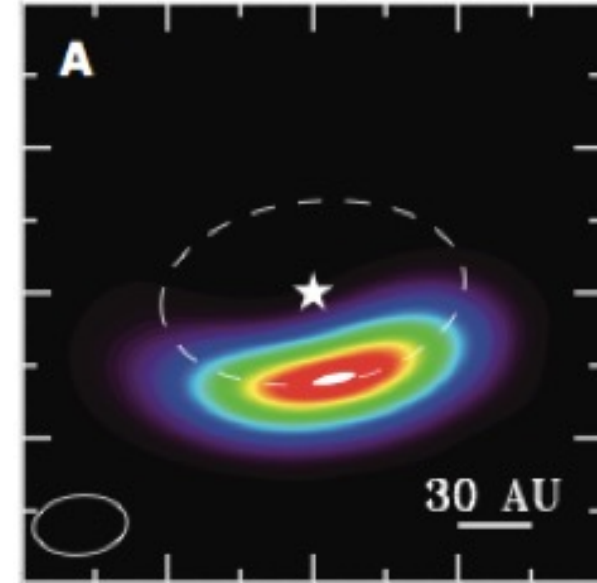
The ALMA Partnership et al. (2015)

SAO 206462



Muto et al. (2012)

Oph IRS 48



van der Marel et al. (2013)

The Atacama Large (sub-)Millimeter Array (ALMA)

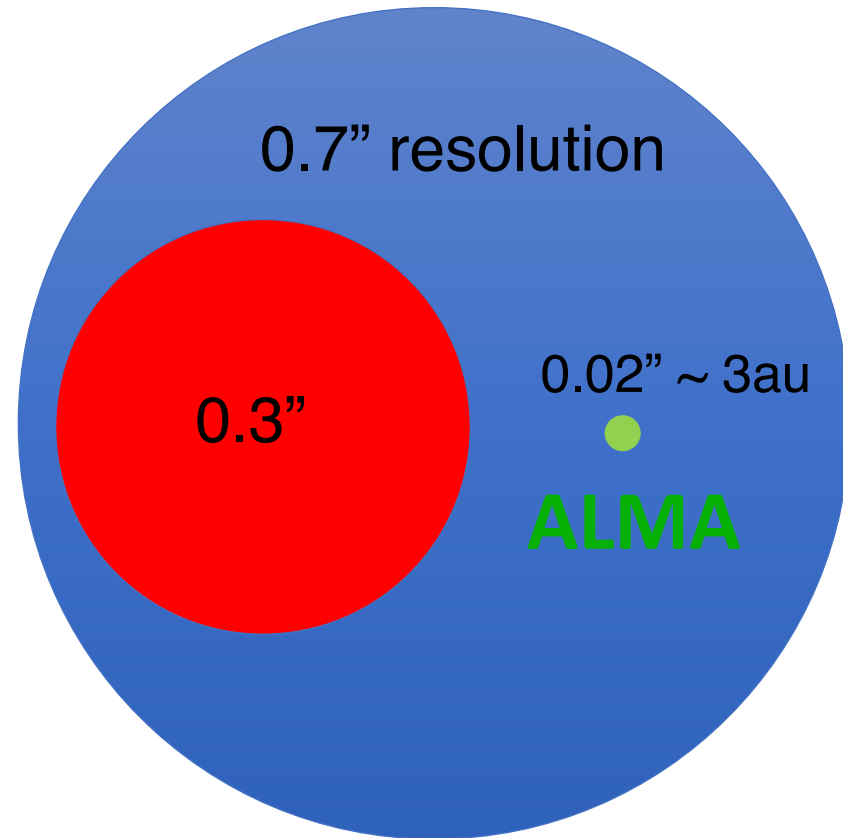
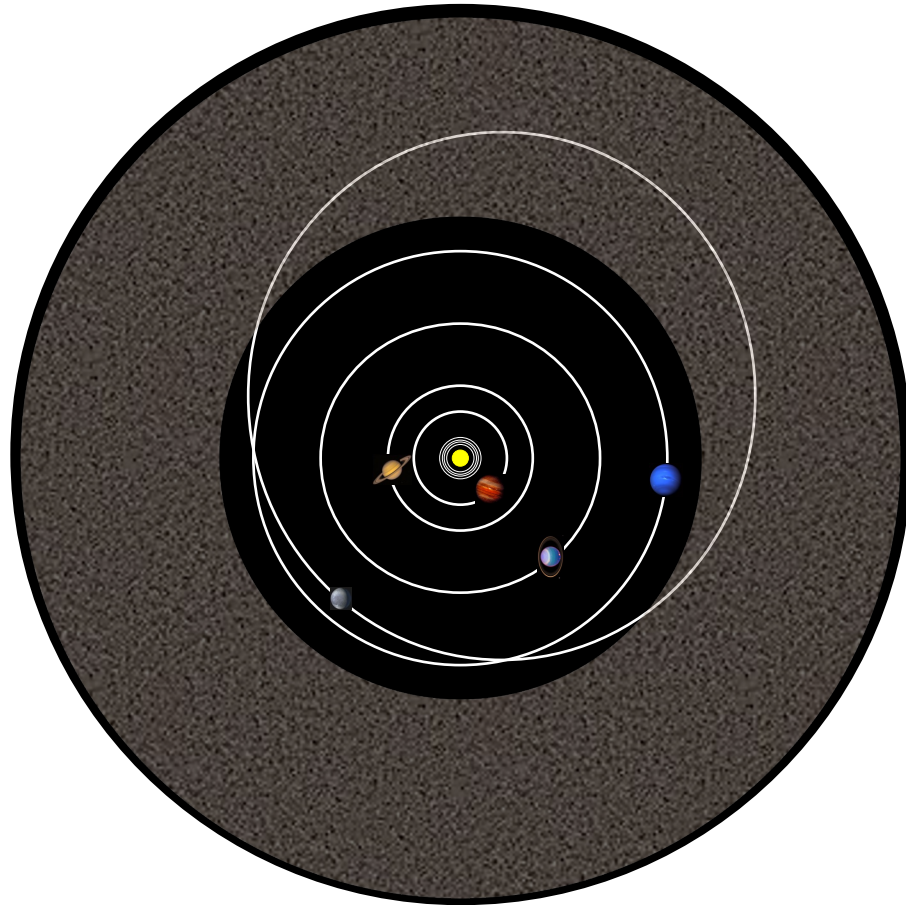


The Very Large Array (VLA)

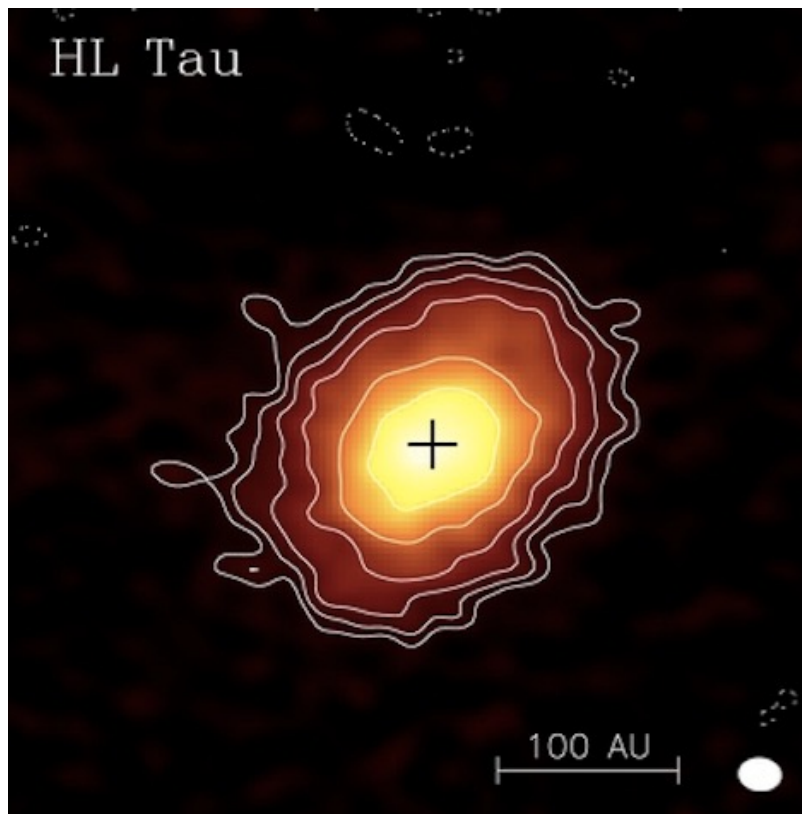


The ALMA ~~Re~~volution

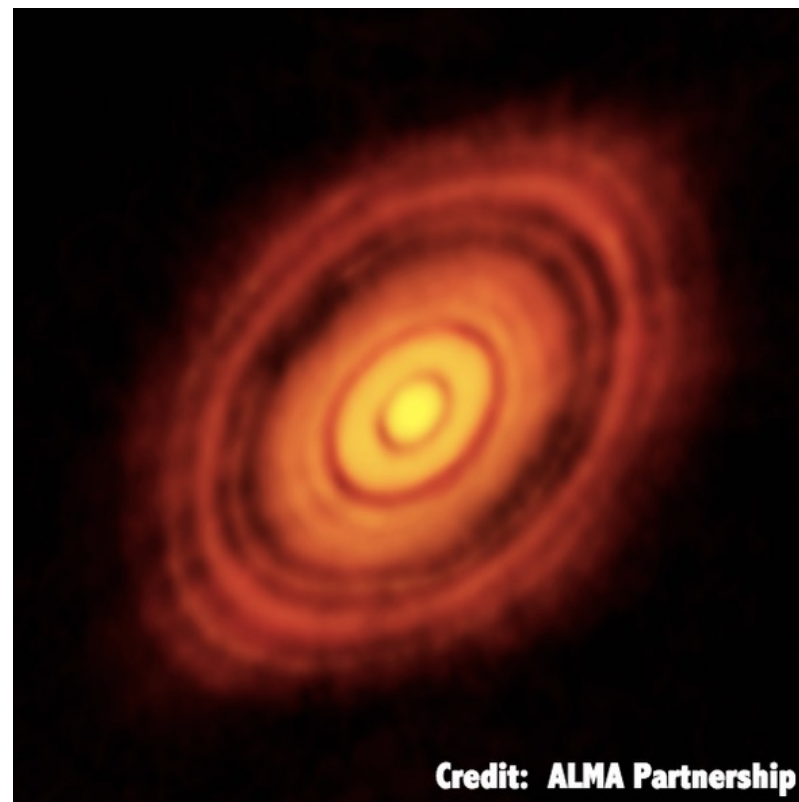
At 140 pc



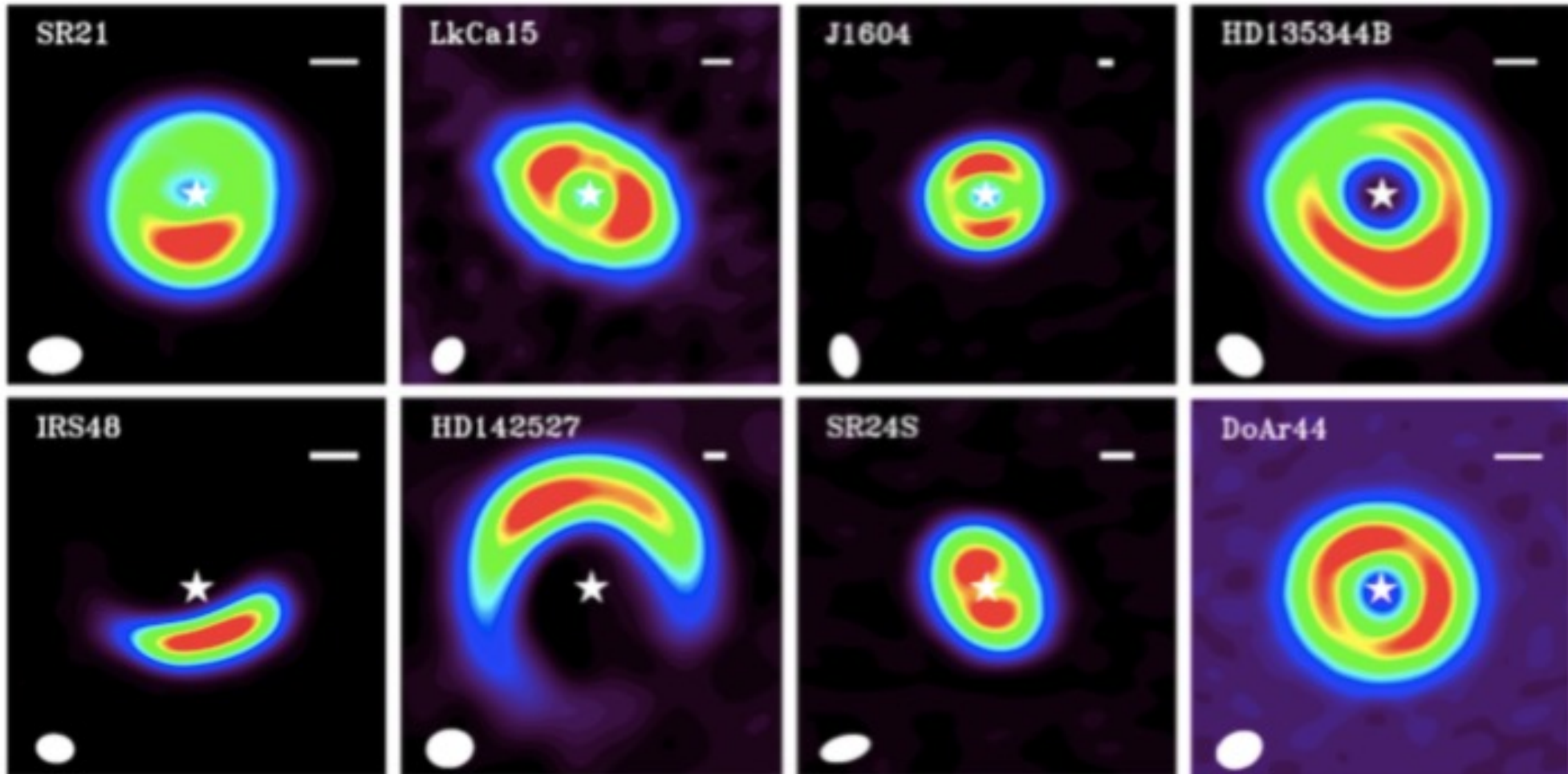
Before ALMA

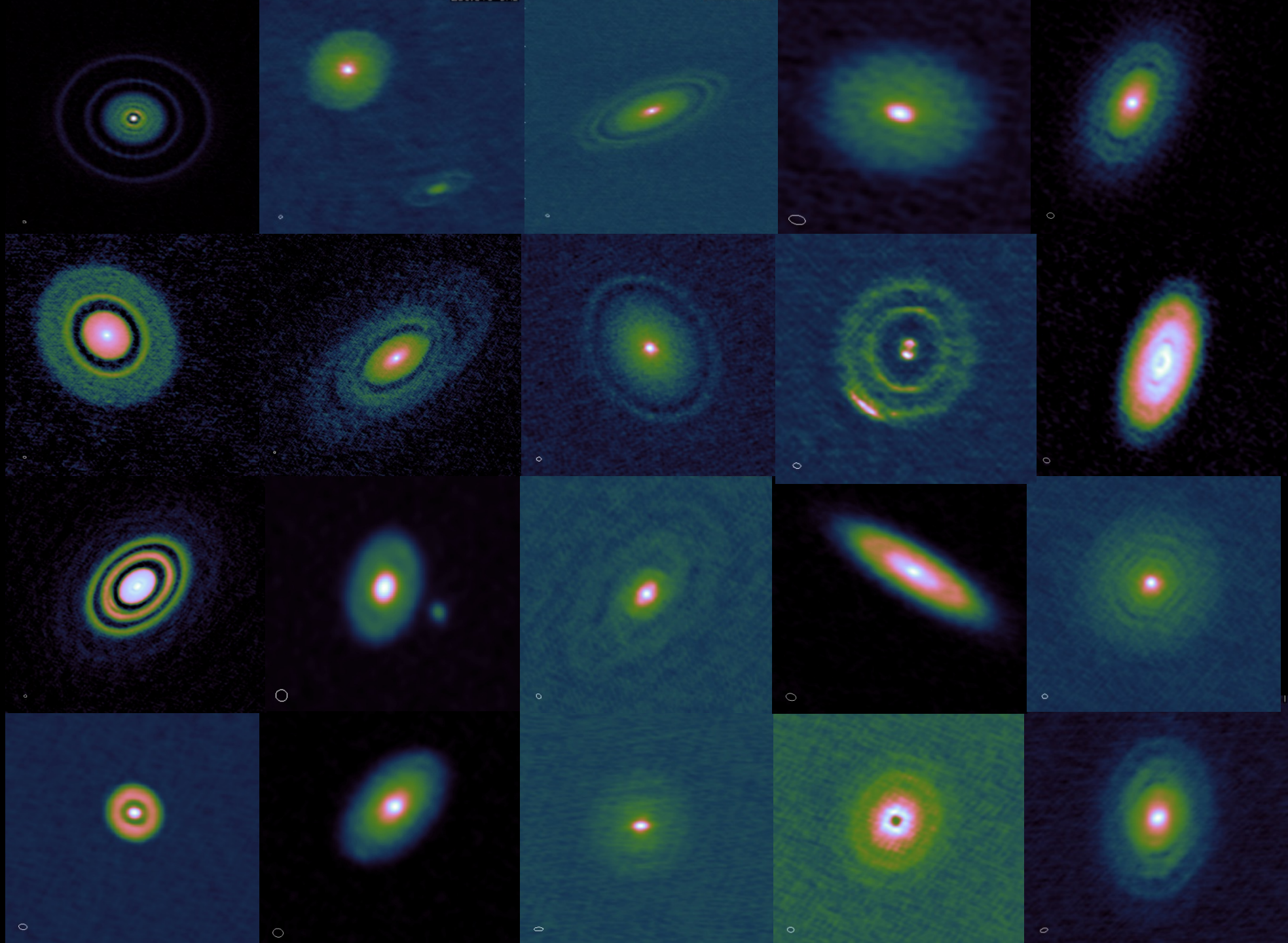


ALMA



Dust traps in disks: ALMA Cycle 0 (2012)





Oph IRS 48



A Major Asymmetric Dust Trap in a Transition Disk

Nienke van der Marel,^{1*} Ewine F. van Dishoeck,^{1,2} Simon Bruderer,² Til Birnstiel,³ Paola Pinilla,⁴ Cornelis P. Dullemond,⁴ Tim A. van Kempen,^{1,5} Markus Schmalzl,¹ Joanna M. Brown,³ Gregory J. Herczeg,⁶ Geoffrey S. Mathews,¹ Vincent Geers⁷

The statistics of discovered exoplanets suggest that planets form efficiently. However, there are fundamental unsolved problems, such as excessive inward drift of particles in protoplanetary disks during planet formation. Recent theories invoke dust traps to overcome this problem. We report the detection of a dust trap in the disk around the star Oph IRS 48 using observations from the Atacama Large Millimeter/submillimeter Array (ALMA). The 0.44-millimeter-wavelength continuum map shows high-contrast crescent-shaped emission on one side of the star, originating from millimeter-sized grains, whereas both the mid-infrared image (micrometer-sized dust) and the gas traced by the carbon monoxide 6-5 rotational line suggest rings centered on the star. The difference in distribution of big grains versus small grains/gas can be modeled with a vortex-shaped dust trap triggered by a companion.

Although the ubiquity of planets is confirmed almost daily by detections of new exoplanets (1), the exact formation mechanism of planetary systems in disks of gas and dust around young stars remains a long-standing problem in astrophysics (2). In

sciencemag.org SCIENCE VOL 340 7 JUNE 2013

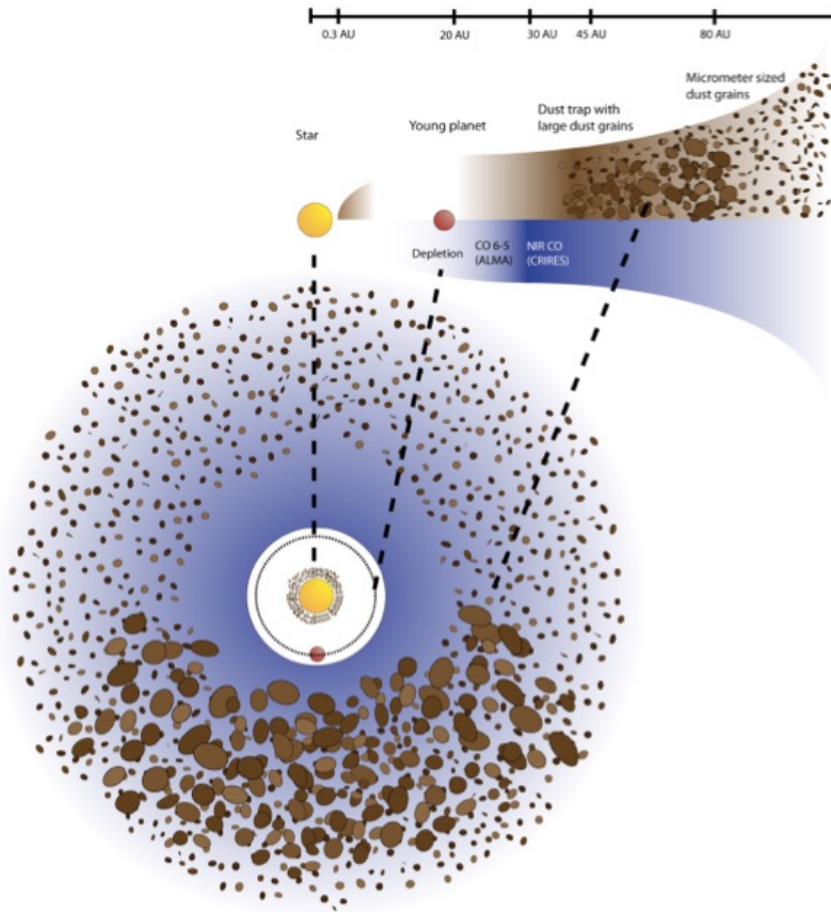
1199

Drawn

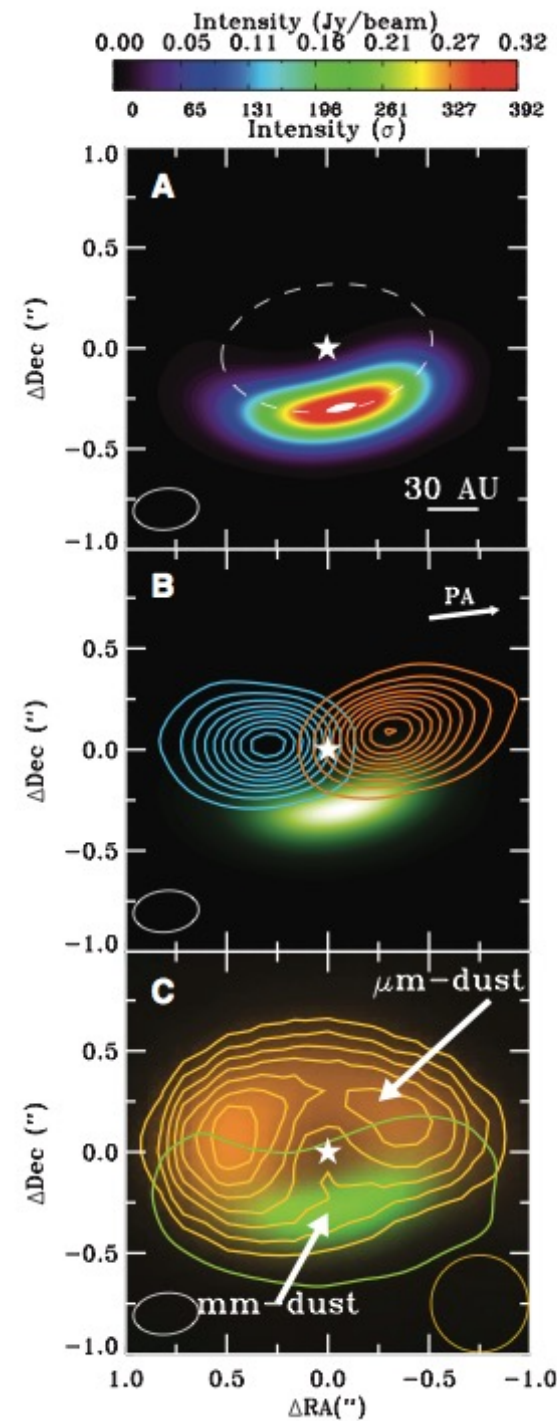
van der Marel+ '13

A huge vortex observed with ALMA

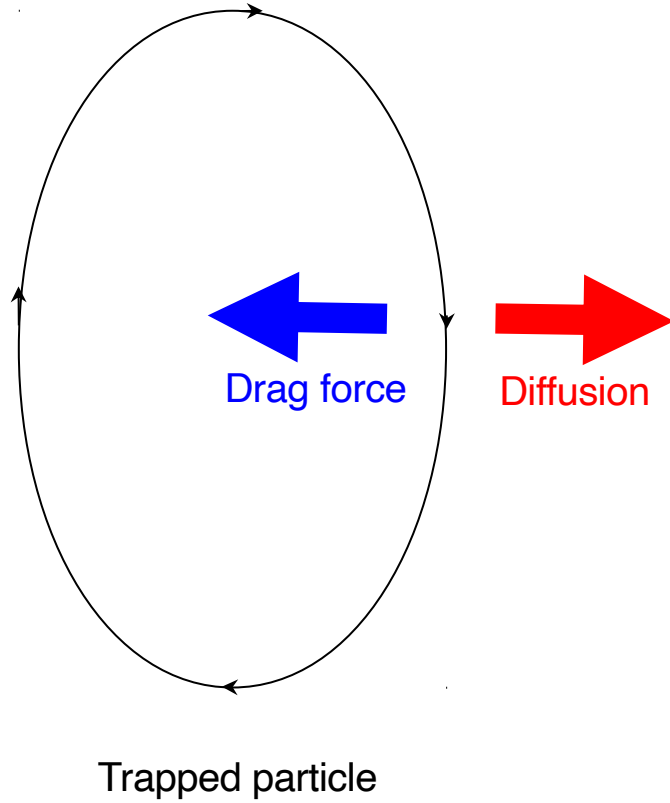
The Oph IRS 48 “comet formation factory”



van der Marel+. '13



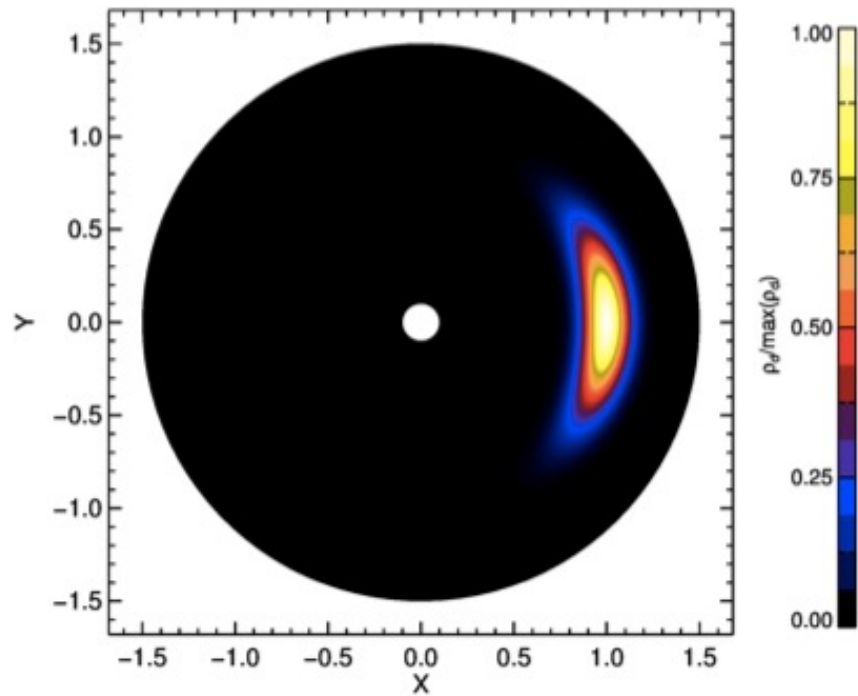
Drag-Diffusion Equilibrium



Dust continuity equation

$$\frac{\partial \rho_d}{\partial t} = -(\underbrace{v \cdot \nabla}_{\text{advection}}) \rho_d - \underbrace{\rho_d \nabla \cdot v}_{\text{compression}} + \underbrace{D \nabla^2 \rho_d}_{\text{diffusion}}$$

Analytical Solution for dust in Drag-Diffusion Equilibrium



Solution for

$$H/r=0.1 \quad \chi=4 \quad S=1$$

Steady-state solution

$$\rho_d(a, z) = \varepsilon \rho_0 (S + 1)^{3/2} \exp \left\{ -\frac{[a^2 f^2(\chi) + z^2]}{2H^2} (S + 1) \right\}$$

Lyra & Lin '13

$$S = \frac{St}{\delta}$$

$$\delta = v_{\text{rms}}^2 / c_s^2,$$

- a = vortex semi-minor axis
- H = disk scale height (temperature)
- χ = vortex aspect ratio
- δ = diffusion parameter
- St = Stokes number (particle size)
- $f(\chi)$ = model-dependent scale function

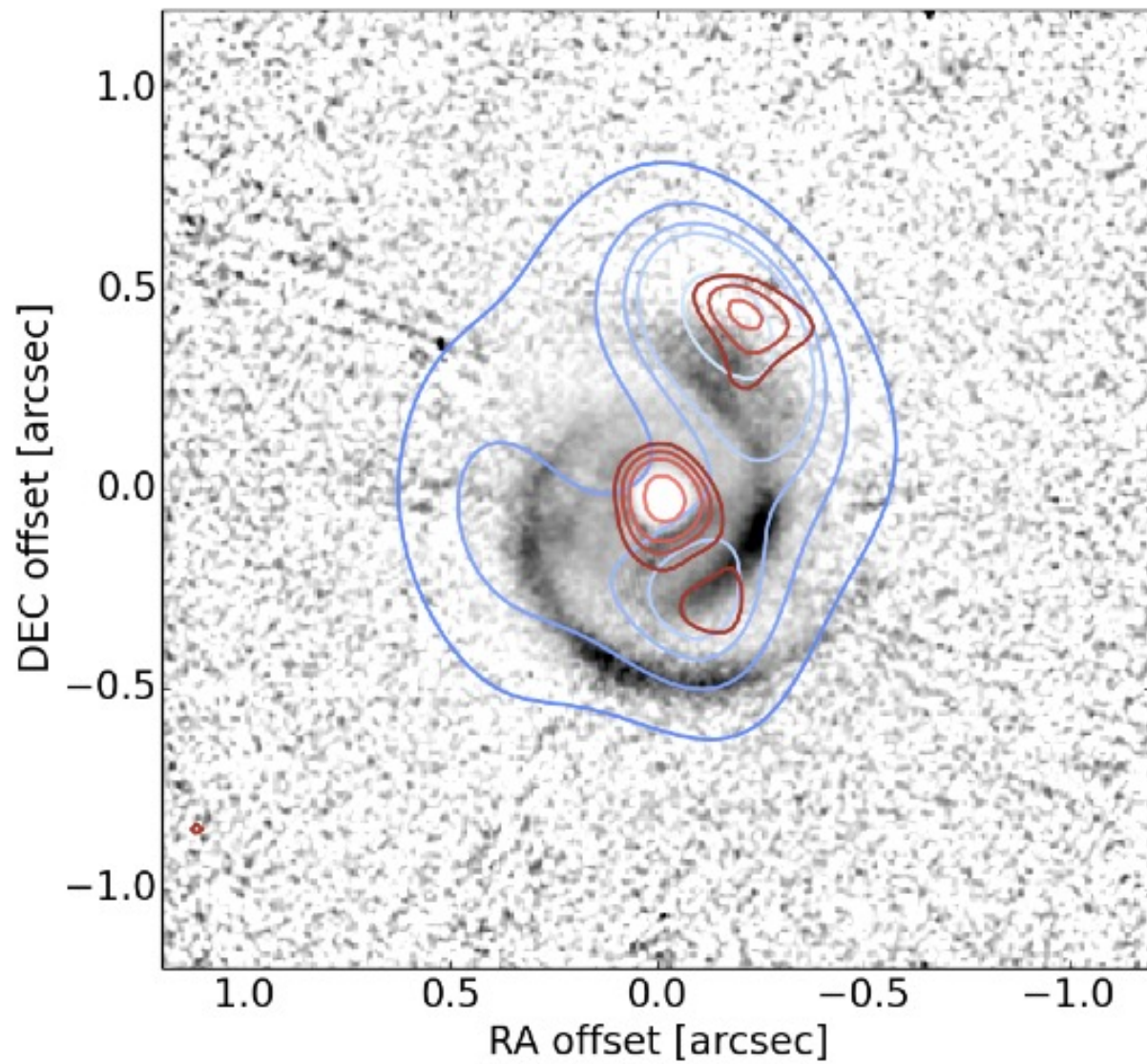
Disk Tomography

SPHERE-ALMA-VLA overlay of MWC 758

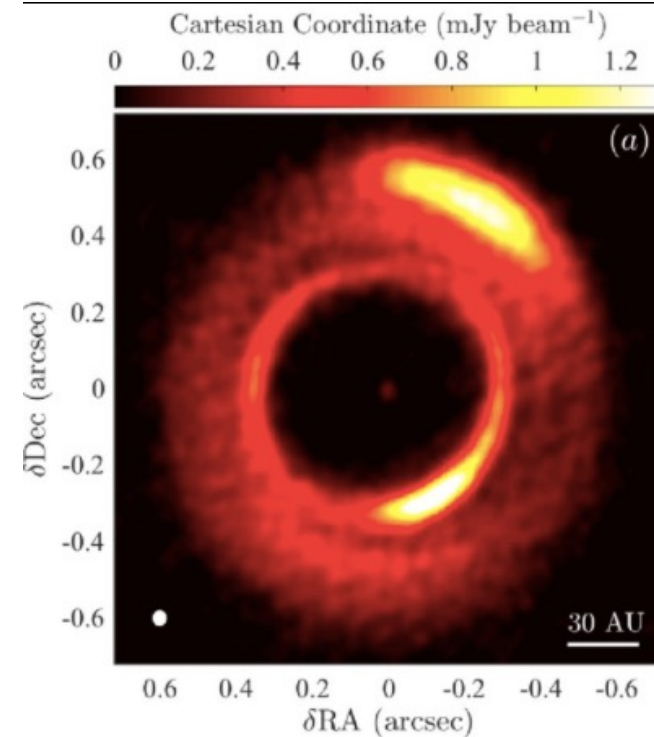
SPHERE (μm)

ALMA ($\sim \text{mm}$)

VLA (cm-m)

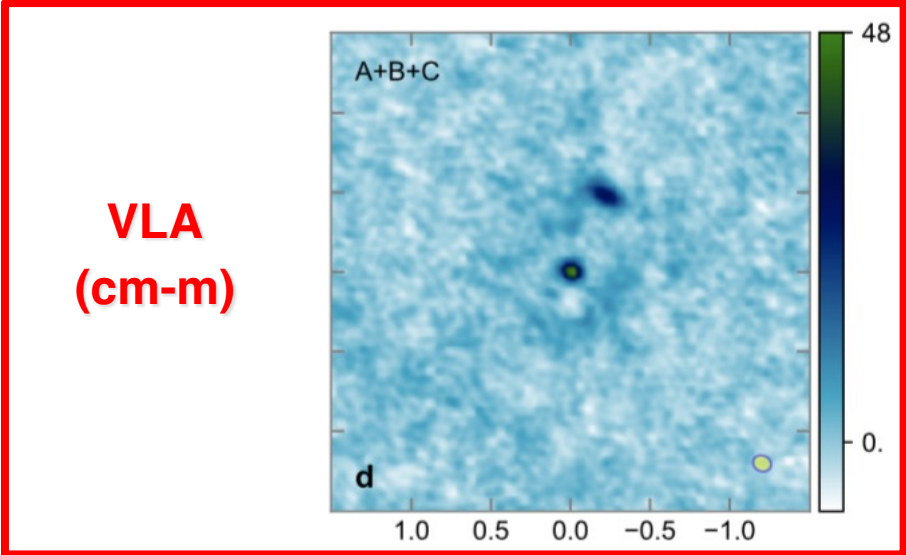
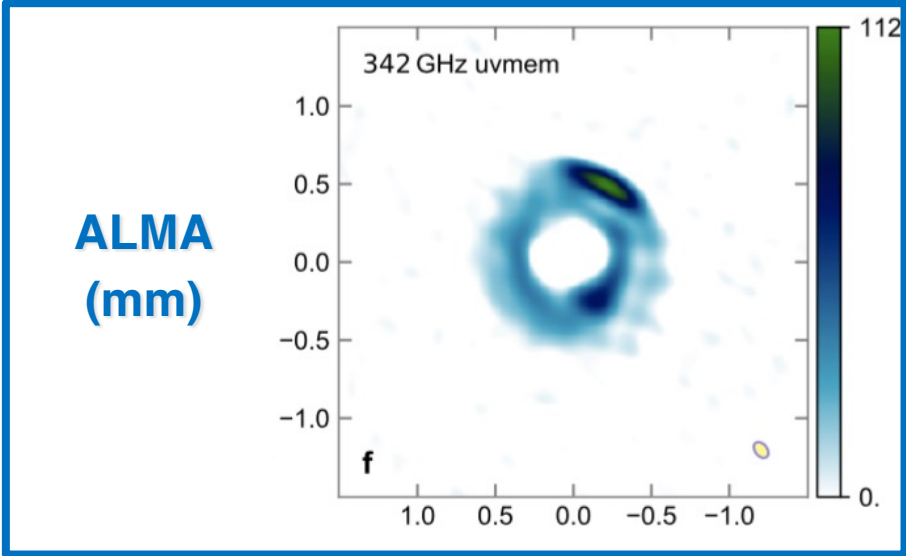


ALMA

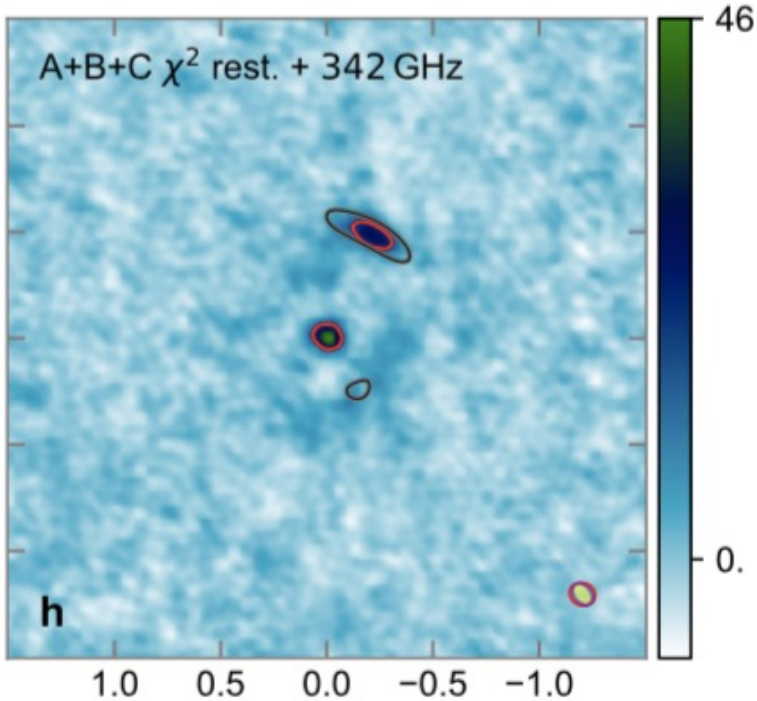


Dong+ '18

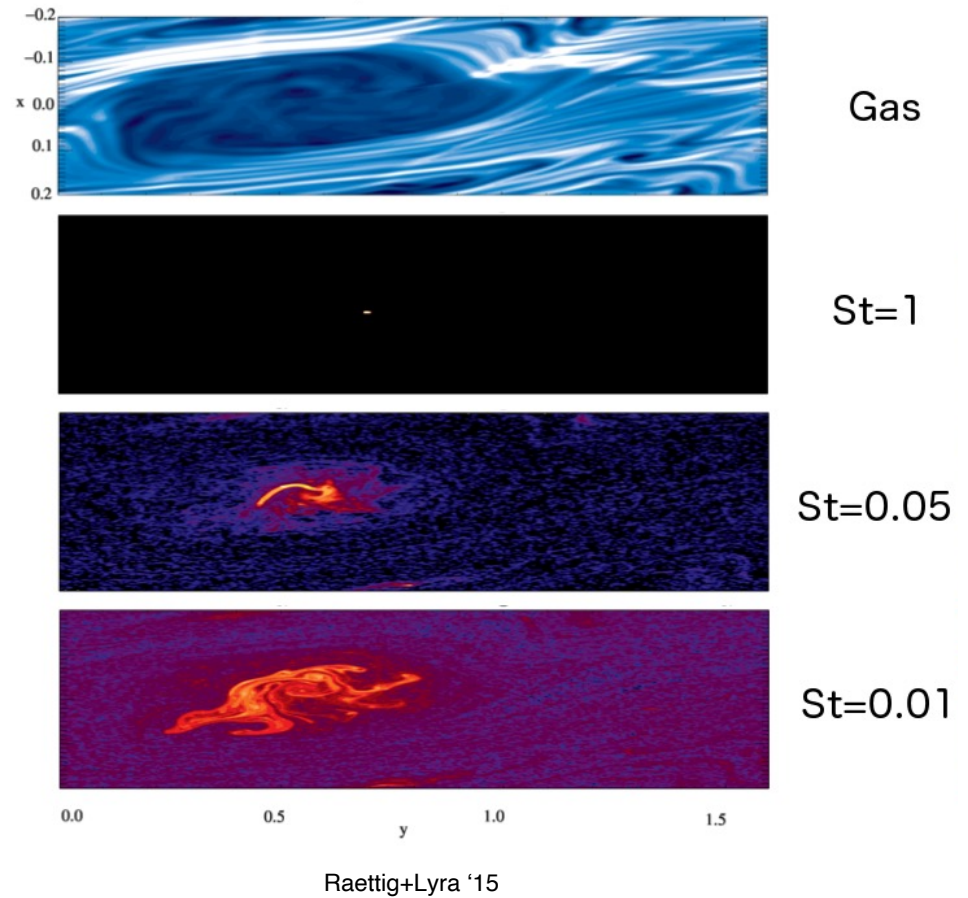
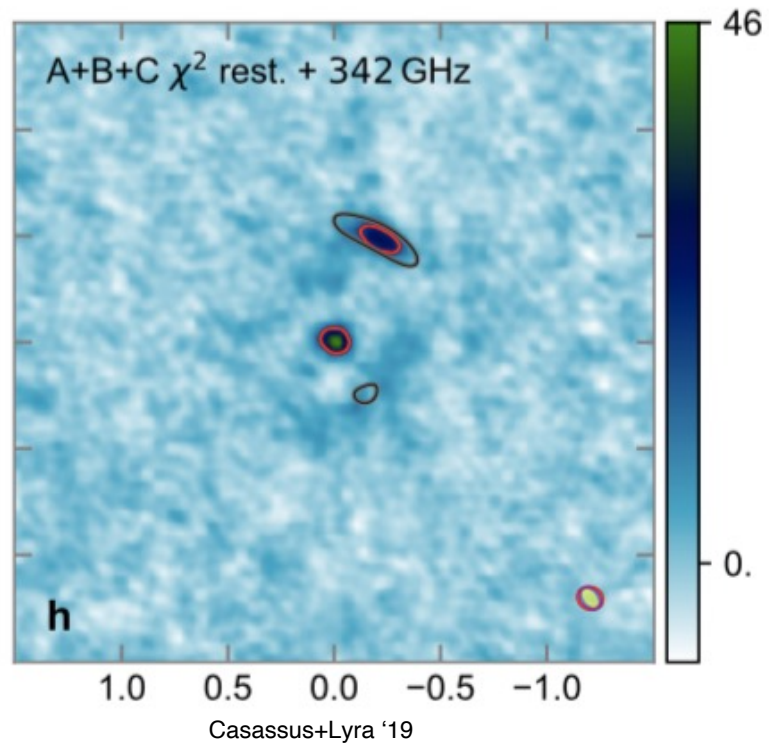
Pebble trapping



Overlay



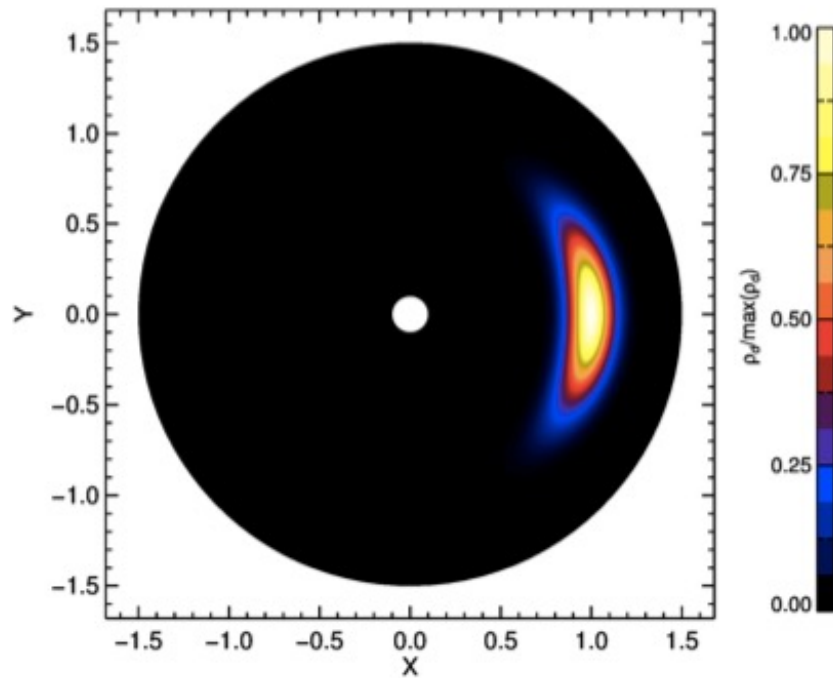
Model vs Observation



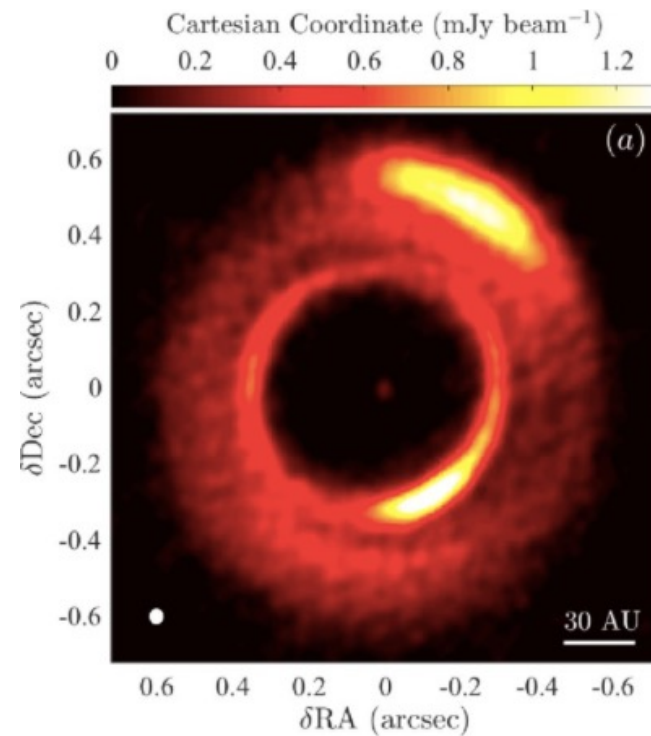
- Vortex-trapped dust in drag-diffusion equilibrium explains the observations

$$\rho_d(a, z) = \epsilon \rho_0 (S + 1)^{3/2} \exp \left\{ -\frac{[a^2 f^2(\chi) + z^2]}{2H^2} (S + 1) \right\}$$

Lyra-Lin solution



Observed Disk



The future

After 10 years of ALMA...

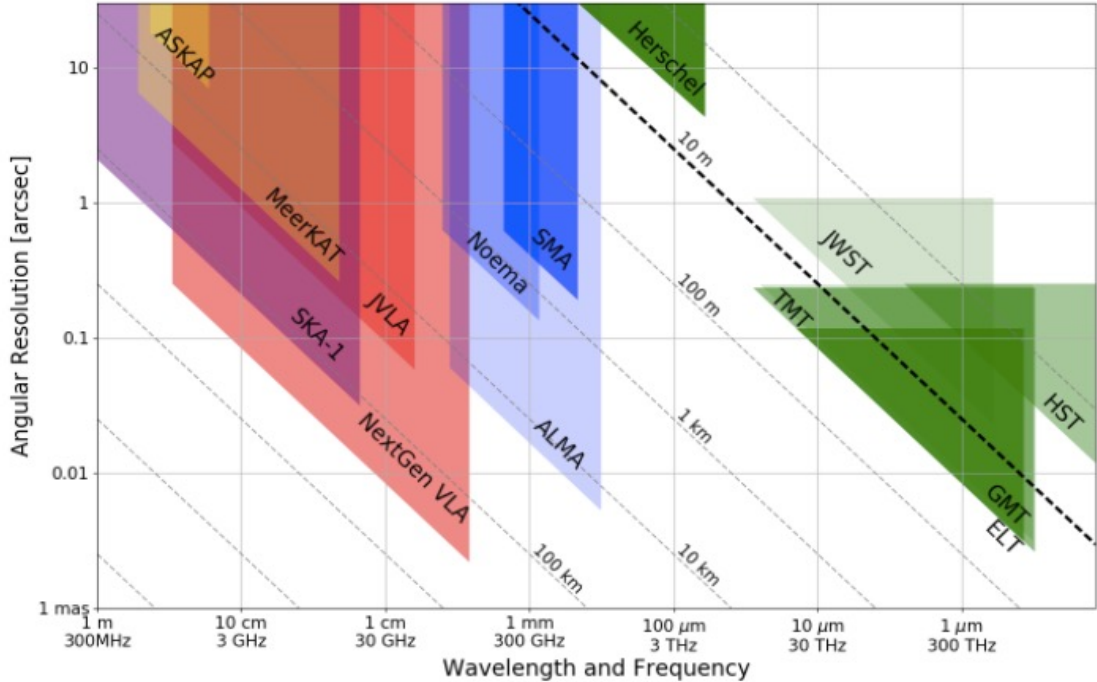
Nearly all nearby disks observed at $<0.1''$ ($< 20\text{-}30\text{AU}$) show substructures.

3 main types of substructures

- Crescent-shaped
- Spiral arms
- Rings/Gaps



Next Generation Very Large Array (ngVLA)



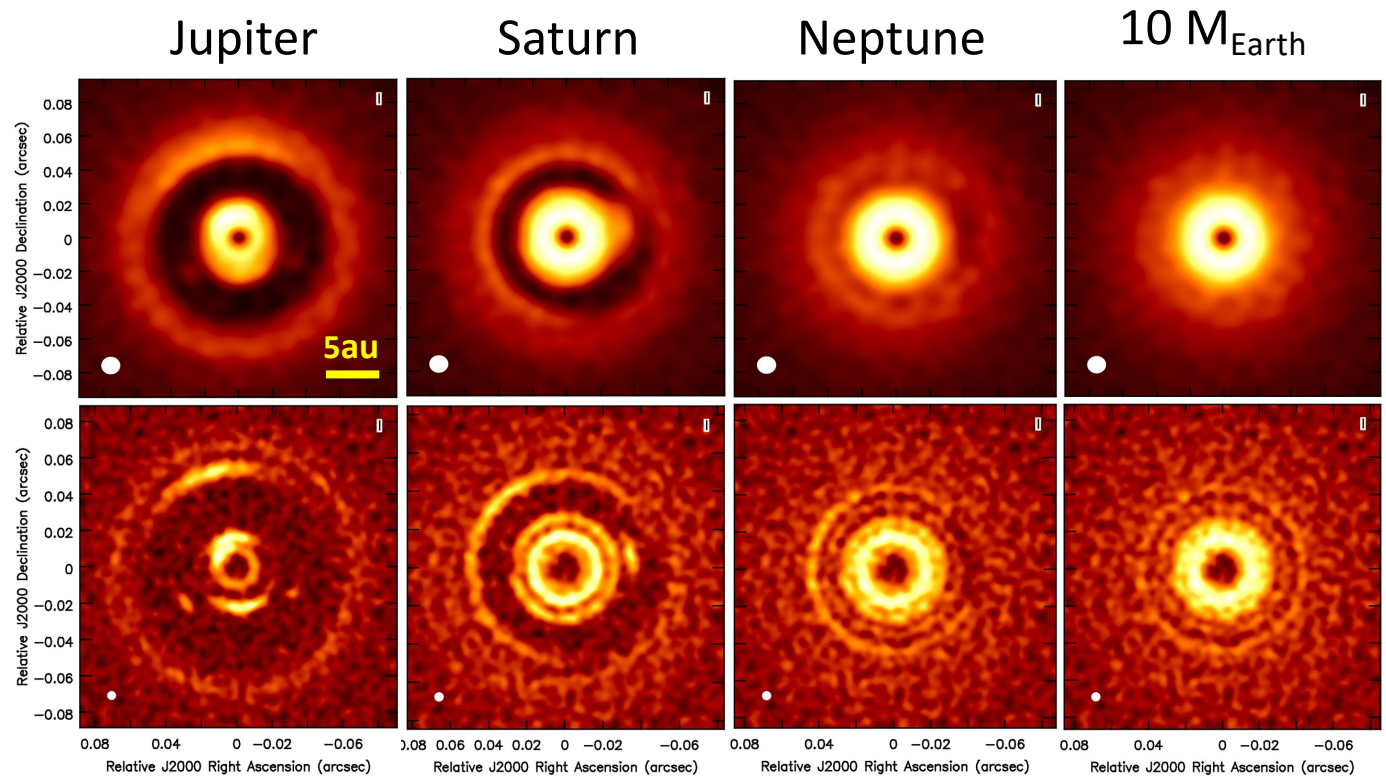
Planets at 5AU

ALMA @ 0.87mm

ngVLA @ 3mm

5 mas = 0.7 AU

rms = 5×10^{-7} Jy/beam

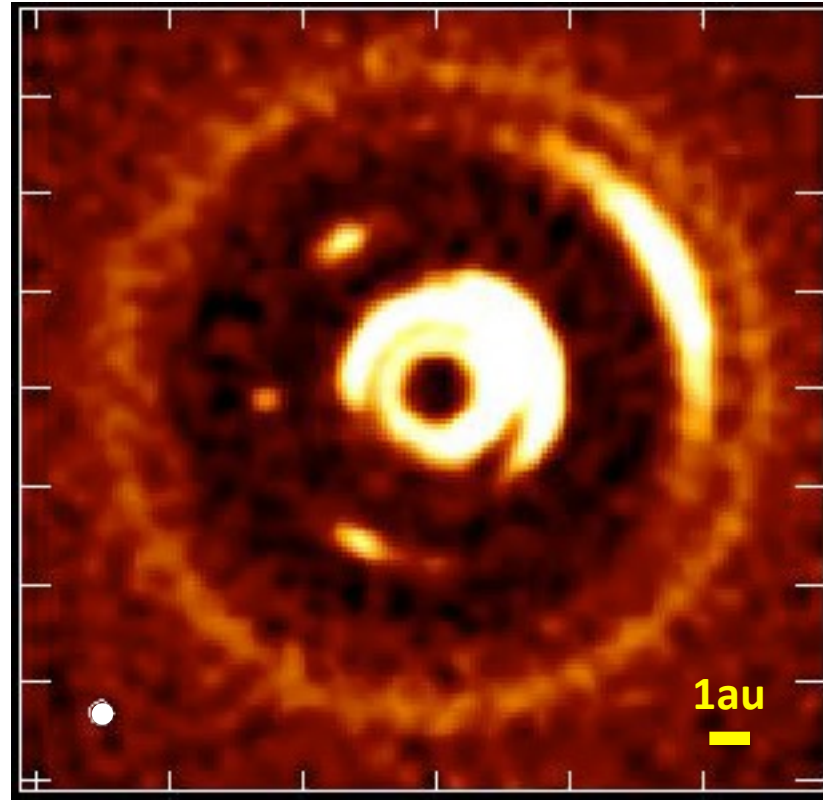


Ricci et al. 2018

ngVLA identifies gaps/substructures down to $\sim 5-10 M_{\text{Earth}}$

ngVLA: Proper motions

Jupiter at 5 AU



Conclusions

- Two routes for planet formation
 - Streaming instability
 - Vortex trapping
- Streaming Instability fits
 - slope of asteroid belt distribution,
 - prograde-retrograde distribution of Kuiper belt objects
 - Low density of small classical Kuiper belt objects
- Pebble accretion is a very efficient planetary growth mechanism
 - Polydisperse Bondi accretion 1-2 orders of magnitude more efficient than monodisperse
 - Silicate pebble accretion explains densities of high-mass Kuiper belt objects
- “Crescents” seen in observations of disks
 - Properties match those of vortices
 - Vortex-trapped dust in drag-diffusion equilibrium explains the observations

**Turbulence and Accretion in 3D Global
MHD Simulations of Stratified Protoplanetary Disk**